CRDV RAPPORT 4196/81
DOSSIER: 7035-BAL
MARS 1981

DREV REPORT 4196/81
FILE: 7035-BAL
MARCH 1981

17KS12000 MOTOR GRAIN STRUCTURAL INTEGRITY ANALYSIS

C. Carrier

Centre de Recherches pour la Défense
Defence Research Establishment
Valcartier, Québec

BUREAU - RECHERCHE ET DEVELOPPEMENT
MINISTERE DE LA DEFENSE NATIONALE
CANADA

RESEARCH AND DEVELOPMENT BRANCH
DEPARTMENT OF NATIONAL DEFENCE
CANADA

CRDV R-4196/81
DOSSIER: 7035-BAL

UNCLASSIFIED

DREV R-4196/81
FILE: 7035-BAL

17KS12000 MOTOR GRAIN

STRUCTURAL INTEGRITY ANALYSIS

by

C. Carrier

CENTRE DE RECHERCHES POUR LA DEFENSE

DEFENCE RESEARCH ESTABLISHMENT

VALCARTIER

Tel: (418) 844-4271

Québec, Canada

March/mars 1981

NON CLASSIFIE

RESUME

Dans le cadre d'une entente prévoyant l'échange de services entre la Bristol Aerospace Ltd. et le Ministère de la défense nationale, on a demandé au Centre de recherches pour la défense de Valcartier d'analyser, entre autres, l'intégrité structurale du pain de propergol du moteur-fusée d'apogée 17KS12000. Lors de l'analyse finale, trois conditions de chargement furent considérées: la contraction thermique, l'accélération au lancement, et la mise sous pression à l'allumage.

L'analyste s'est servi de la méthode des éléments finis et a appliqué la technique des variables réduites de Williams-Landel-Ferry aux propriétés mécaniques du propergol. (NC)

ABSTRACT

As part of a Provision of Services Agreement between Bristol Aerospace Ltd. and the Department of National Defence, the Defence Research Establishment, Valcartier was required to perform the structural integrity analysis of the grain of a solid propellant rocket motor, designated as the 17KS12000. Three load cases were considered for the final analysis: thermal contraction, launch acceleration, and ignition pressurization.

The analyst used the finite element method and applied the Williams-Landel-Ferry technique of reduced variables to the propellant mechanical properties. (U)

TABLE OF CONTENTS

NOMENCLATURE

Symbols

a_T	WLF time-temperature shift factor
BFZ	Computer input mnemonic for the axial body force (lb_f/in^3) on the propellant
BFZC	Computer input mnemonic for the axial body force (lb_f/in^3) on the casing
E	Initial slope modulus (psi)
GL	Effective gage length (3.32 in for JANNAF specimens)
[i,j]	Element i-j
(i,j)	Node i-j
R	Crosshead speed (in/min)
T	Temperature (K)
T_c	Propellant cure temperature
T_1	Zero-strain temperature
t	Time (min)
THERM	Mnemonic for the total thermal contraction (in/in) of the propellant
THERMC	Mnemonic for the total thermal contraction (in/in) of the casing
α_c	Coefficient of thermal expansion (in/in ^oF) of the casing
α_p	Coefficient of thermal expansion (in/in ^oF) of the propellant
ε_m	Strain at maximum load (in/in)
$\lambda_m = 1 + \varepsilon_m$	Extension ratio at maximum load

σ	Standard deviation
σ_m	Nominal stress at maximum load (psi)
σ_r	Radial stress (psi)
τ_m	Maximum shear stress (psi)

ABBREVIATIONS

BAL	Bristol Aerospace Ltd.
DND	Department of National Defence
DREV	Defence Research Establishment, Valcartier
HTPB	Hydroxyl-Terminated Polybutadiene
NASA	National Aeronautics and Space Administration
WLF	William-Landel-Ferry
SCF	Strain concentration factor
SF	Safety factor

1.0 INTRODUCTION

In early 1979, the National Aeronautics and Space Administration (NASA) contracted Bristol Aerospace Ltd. (BAL) for the development of a solid propellant rocket motor to be adapted as a third-stage motor to the Terrier/Black Brant V sounding rocket vehicle. The projected missions required that the motor contain approximately 700 lb of a high-energy, HTPB-based propellant. In order to speed up the developmental work, the contractor decided to use, whenever possible, inert components of the 17-in Black Brant V motor.

Following a Provision of Services Agreement between BAL and the Department of National Defence (DND), the Defence Research Establishment, Valcartier (DREV), was required to perform the grain internal ballistics and structural integrity analyses of the projected motor designated as the 17KS12000.

This report covers the structural integrity analyses of the 17KS12000 propellant grain. The grain analysed herein differs from a preceding design (BAL's DWG 600-03890, dated 10 Oct., 1979): the port diameter is 4.5 in instead of 4.0 in, and the fins of its booster cavity are smoothly blended with the cylindrical port. The previous design was modified after preliminary analyses had indicated that its safety factor was somewhat low.

The structural integrity investigation included structural and failure analyses for the three following load cases:

a. thermal contraction at the lowest operating temperature limit ($-10^{\circ}F$);
b. longitudinal acceleration under launch conditions at high temperature (15 g_n at $110^{\circ}F$);
c. ignition pressurization at low temperature (1 000 psi at $-10^{\circ}F$).

The effects of combined loads were not considered.

A series of two-dimensional, linear, elastic analyses were conducted for each load case, using the finite element method. The critical results of these analyses were subsequently compared to the appropriate failure data. To take into account the thermoviscoelastic nature of the propellant, its appropriate mechanical properties (ε_m, σ_m and E) were treated according to the Williams-Landel-Ferry (WLF) technique, assuming that the time-temperature equivalence principle was valid for the highly loaded, HTPB-based propellant.

To summarize the analyses reported herein, let us say that the modified 17KS12000 design can be considered adequate, since its minimum strain-based safety factor is 1.71.

This work was performed at DREV between December, 1979, and March, 1980, under PCN 21C91, Assistance to BAL.

2.0 GRAIN STRUCTURAL ANALYSES

2.1 Thermal Loading

2.1.1 General

The most severe loading condition this case-bonded, solid-propellant rocket motor can be subjected to is repetitive low-temperature cycling. For the analyses reported herein, the thermal stresses and strains induced in the propellant grain by the difference between the coefficients of thermal expansion of the propellant and the motor case were determined only for a soak of the grain at low temperature. Cumulative damages due to temperature cycling effects were covered by insuring an adequate design safety factor.

Special attention was given to:

a) the hoop strain at the inner bore, espacially at the finocyl transition region,
b) the hoop strain at the star tip of the booster cavity,
c) the stresses at the case-grain termination points,
d) the stresses at the case-grain interface at the motor mid-length.

The lower operating temperature limit was specified as:

$$T_{low} = -10^{o}F \ (250 \ K) \qquad [1]$$

2.1.2 Heat Transfer Analysis

An elementary heat transfer analysis, not reported herein, indicated that the response time of the motor to a temperature drop was approximately 2 300 min. For the structural analysis, this was considered as the effective cooling time.

$$t_{cooling} \simeq 2\ 300 \text{ min} \qquad [2]$$

The heat transfer analysis also showed that the usual assumption of a uniform temperature distribution throughout the grain during cooling was warranted, for engineering practicality.

2.1.3 Cure shrinkage and Thermal Contraction of the Grain

The effects of the cure shrinkage of the propellant were also included in the thermal contraction. For that purpose, the thermal strain calculations were referred to the zero-strain temperature, T_1, which is typically $15^{o}F$ higher than the cure temperature T_c, for polybutadiene propellant (Ref. 1). Thus

$$T_1 = T_c + 15^{\circ}F$$

$$= 140 + 15 = 155^{\circ}F \qquad [3]$$

Then, equivalent thermal contractions were calculated using an equivalent temperature change of

$$\Delta_T = T_{low} - T_1$$

$$= -10 - (155) = -165^{\circ}F \qquad [4]$$

With α_p and α_c taken from Table I, it follows that the total thermal strain of the propellant is

$$THERM = \alpha_p \Delta T$$

$$= 5.86 \times 10^{-5} \times (-165)$$

$$= -0.967 \times 10^{-2} \frac{in}{in} \qquad [5]$$

and that the total strain of the casing is

$$THERMC = \alpha_c \Delta T$$

$$= 11.7 \times 10^{-6} \times (-165)$$

$$= -1.93 \times 10^{-3} \frac{in}{in} \qquad [6]$$

TABLE I

Relevant Mechanical & Physical Properties

Properties	Symbol	Unit	Casing Steel AMS6435	Propellant	Insulant RF/B
Coeff. of Thermal Expansion	α	$\frac{in}{in^{o}F}$	11.7×10^{-6}	5.86×10^{-5}	N.A.
Specific Weight	γ	$\frac{lb}{in^{3}}$	0.283	0.0647	N.A.
Young's Modulus	E	psi	29×10^{6}	(Fig. 1)	N.A.
Poisson's Ratio	ν	-	0.29	0.491 (estimated)	N.A.
Thermal Conductivity	k	$\frac{BTU}{in^{o}F\ s}$	3.86×10^{-4}	3.29×10^{-6}	4.9×10^{-6}
Specific Heat	c_p	$\frac{BTU}{lb^{o}F}$	-	0.31 (estimated)	N.A.

2.1.4 Thermoviscoelastic Properties of the Propellant

To take into account the thermoviscoelastic nature of the propellant, the gross data from the uniaxial tension tests conducted at various crosshead speeds and temperatures were reduced according to the WLF technique (Ref. 2). Appendix A lists the equations used to perform these reductions, and Figs. 1 to 3 show the reduced data with appropriate lower and/or upper limits.

The mechanical properties necessary for the structural analyses of the thermal loading were calculated as follows: a reduced cooling time was computed using eqs. A-1 and A-3

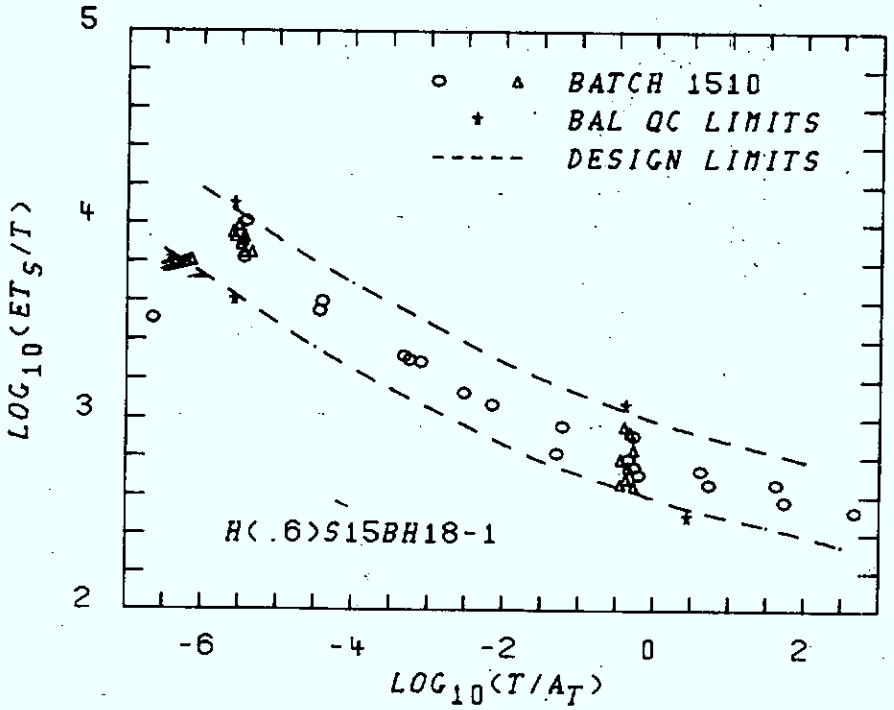

FIGURE 1 - Reduced Modulus vs Reduced Time

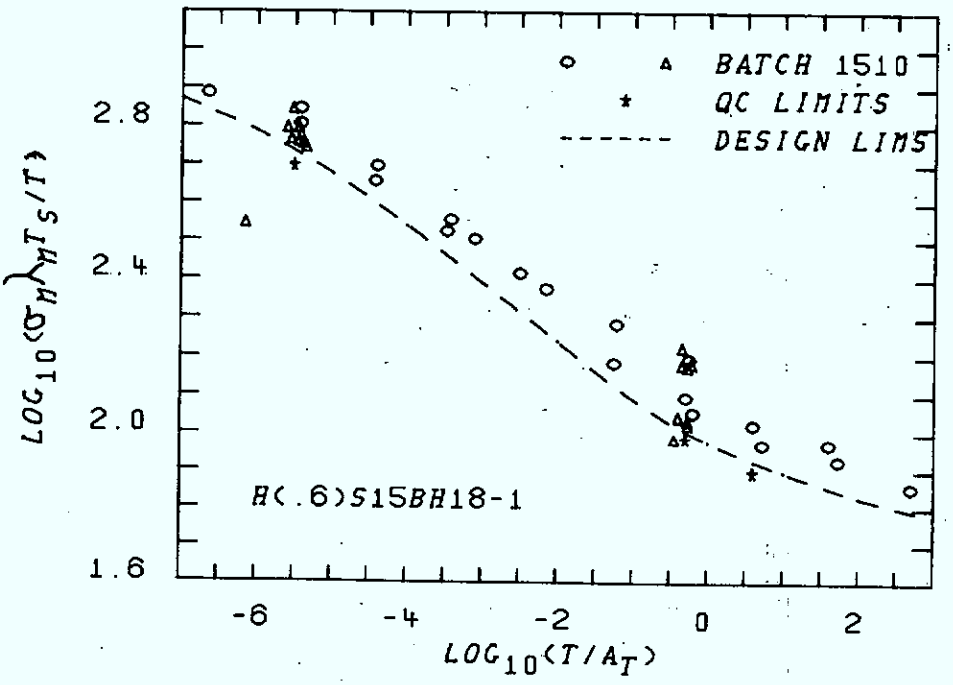

FIGURE 2 - Reduced Stress vs Reduced Time

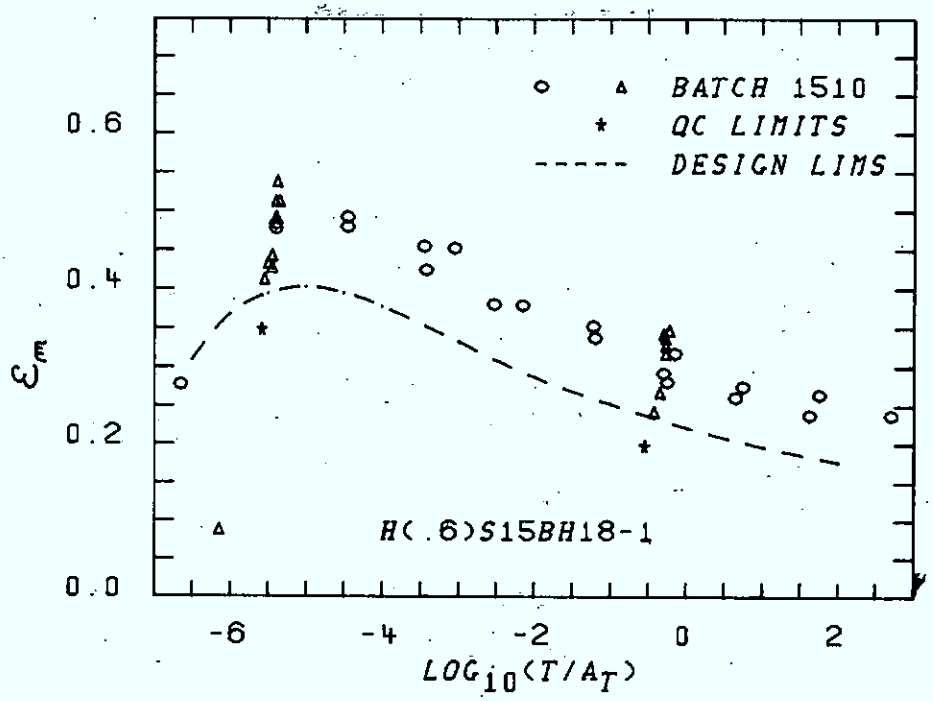

FIGURE 3 - Maximum Strain vs Reduced Time

$$\log \frac{t}{a_T} = \log t - \log a_T \qquad [A\text{-}1]$$

$$\log a_T = \frac{-8.86\ (T-239)}{T-137.4} + 3.18 \qquad [A\text{-}3]$$

With t = 2 300 min, the estimated cooling time, and T = 250 K, the lower operating temperature limit, we obtain

$$\log \frac{t}{a_T} = \log 2300 - \left[\frac{-8.86\ (250-239)}{250 - 137.4} + 3.18 \right]$$

$$= 1.05 \qquad [7]$$

At a reduced time of 1.05, the upper limit of the propellant reduced modulus is 2.88 (Fig. 1), hence

$$E = 639 \text{ psi;} \qquad [8]$$

the lower limit of the maximum strain capability is (Fig. 3)

$$\varepsilon_m = 0.20 \qquad [9]$$

and the lower limit of the reduced maximum stress is 1.89 (Fig. 2), hence

$$\sigma_m = 54.5 \text{ psi.} \qquad [10]$$

2.1.5 Finite Element Model

In accordance with the approach commonly employed throughout the solid rocket industry, the modeling of the three-dimensional 17KS12000 motor grain was done by performing a series of two-dimensional analyses, namely:

a) a longitudinal, axisymmetric analysis of the complete grain, for which we considered the booster cavity as a cylinder whose radius is equal to that of a circle circumscribing the star tips of the booster cavity (Figs. 4a, b, and c).

b) two transverse, plane strain analyses of the booster cavity: one of the actual cross section (Fig. 5a) and the other of the idealized axisymmetric cross section (Fig. 5b). Comparing the results of both analyses permitted us to calculate a strain concentration factor (SFC) at the fin tips. This SCF was then applied to the maximum hoop strain calculated during the first axisymmetric analysis (Figs. 4a, b, and c).

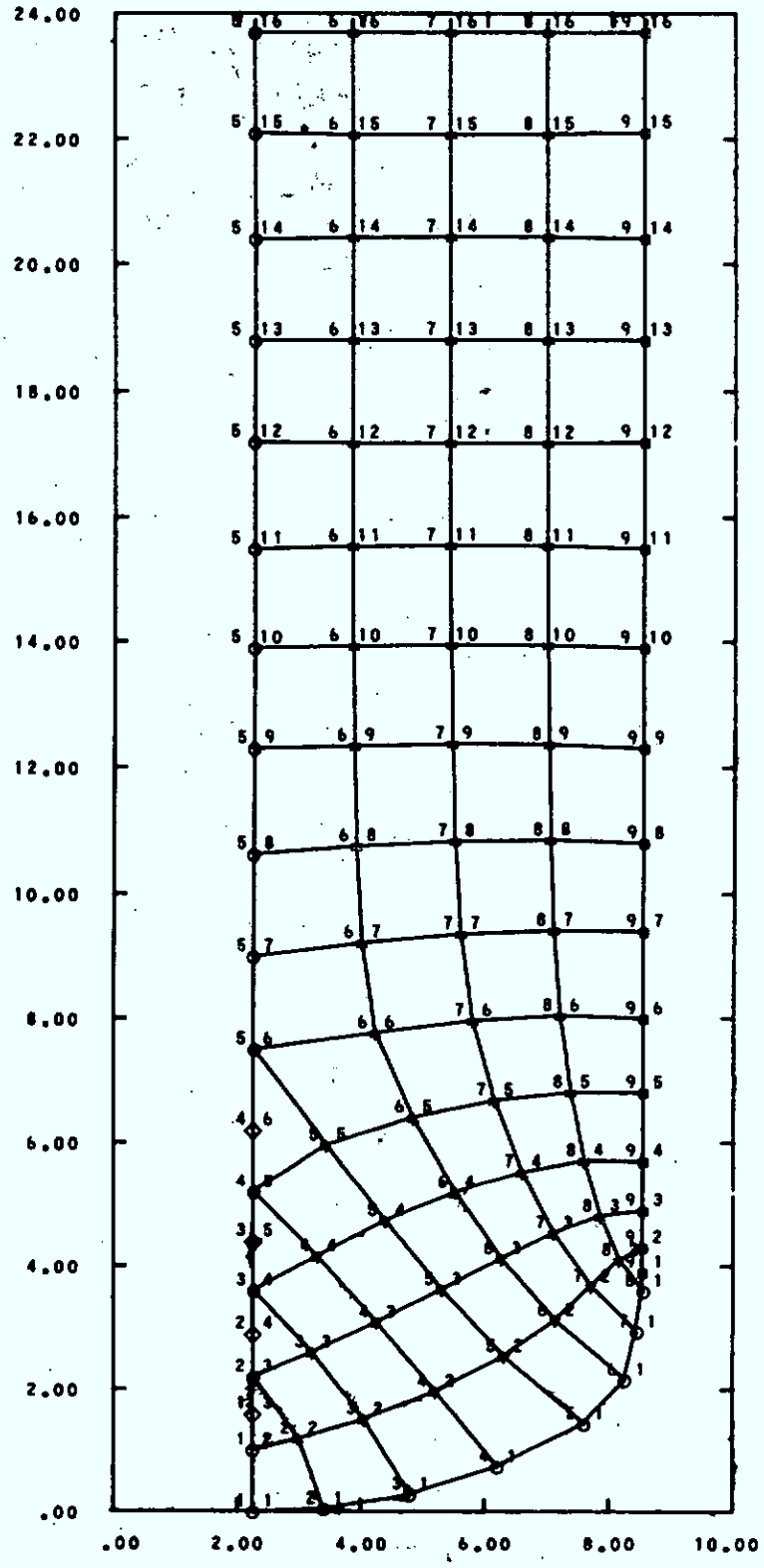

FIGURE 4a - Axisymmetric Finite Element Model: Motor Head-End

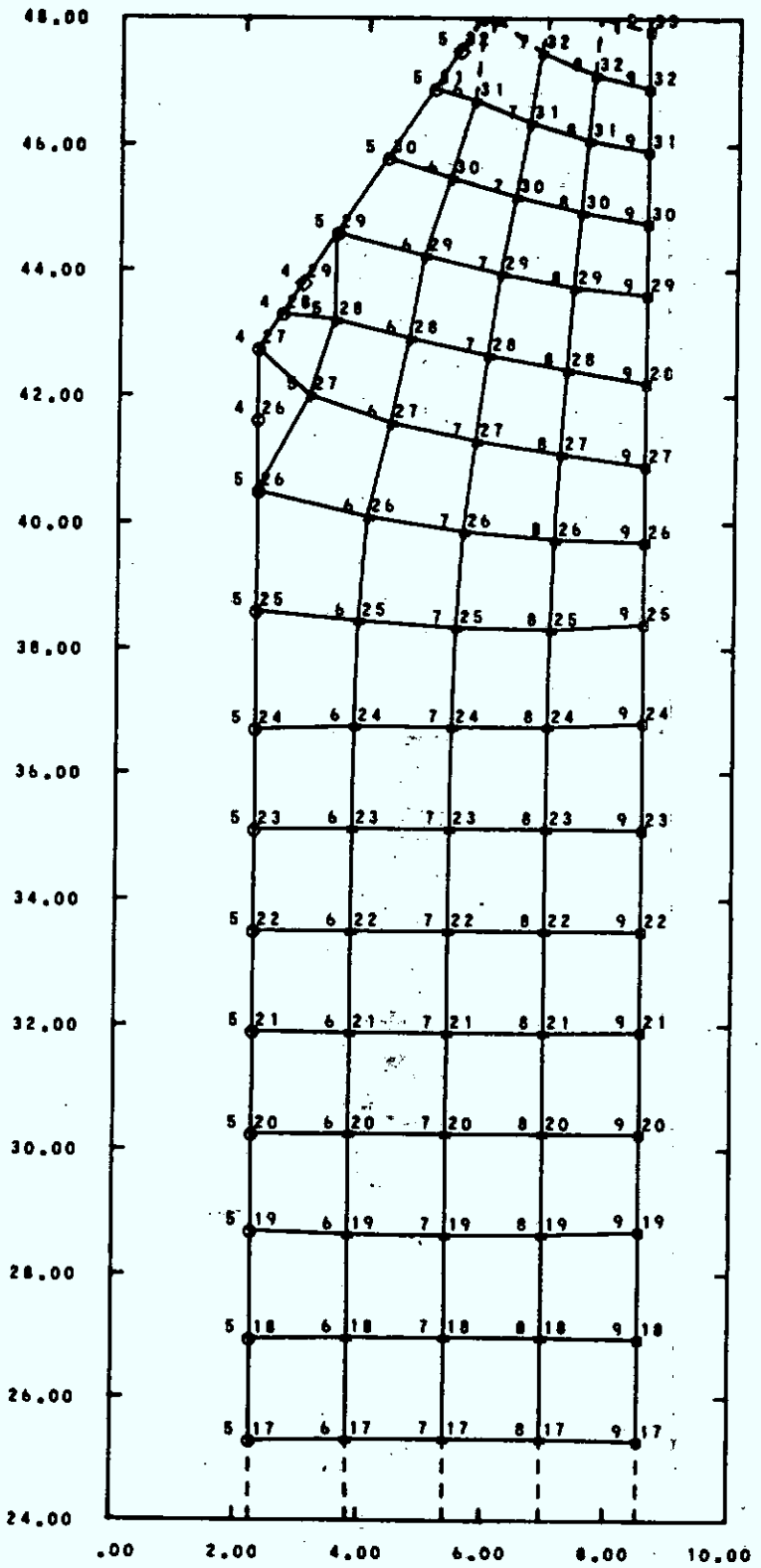

FIGURE 4b - Axisymmetric Finite Element Model: Motor Mid-Section

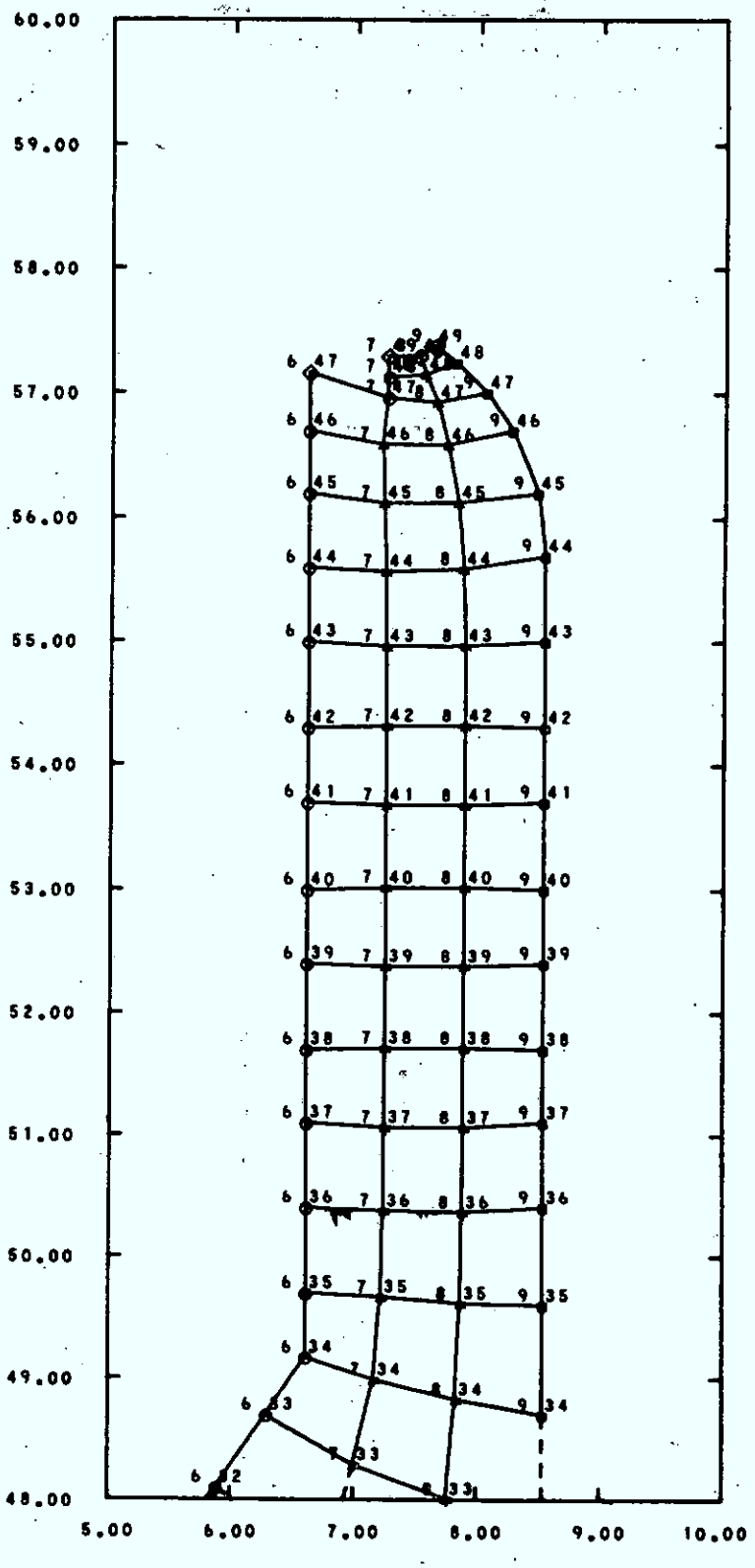

FIGURE 4c - Axisymmetric Finite Element Model: Motor Nozzle-End

c) a circumferential, plane stress analysis of the inner surface of the port, at the finocyl transition region (Fig. 6), to compute the SCF at this particular location. This SCF was then applied to the transition hoop strain computed during the first axisymmetric analysis to evaluate the actual maximum strain in this area.

The analyses were performed using AMG032 and AMG033, parts of a package written by Rohm & Haas Ltd. (Ref. 3) for grain structural analysis using the finite element method.

2.1.6 Results

1) The SCF at the finocyl transition was computed as

$$SCF = \frac{\text{max. strain [5,10]}}{\text{max. strain [1,1]}}$$

$$= \frac{0.13568}{0.091245} = 1.487 \qquad [11]$$

where 5,10 and 1,1 stand for the appropriate elements. Pertinent pages of the computer outputs are included as Appendix B, and Figs. 7a and b illustrate the results.

2) When extrapolated to the surface, the plane strain analysis of the actual cross section of the motor cavity (Fig. 8a and Appendix C-1) indicated a maximum strain of 0.037742 for the element [1,2] (See note p. 20). A similar analysis of the idealized axisymmetrix booster cavity (Fig. 8b and Appendix C-2) yielded a maximum strain of 0.008884 for the element [1,1]. Therefore,

$$SCF = \frac{0.037742}{0.008884} = 4.25 \qquad [12]$$

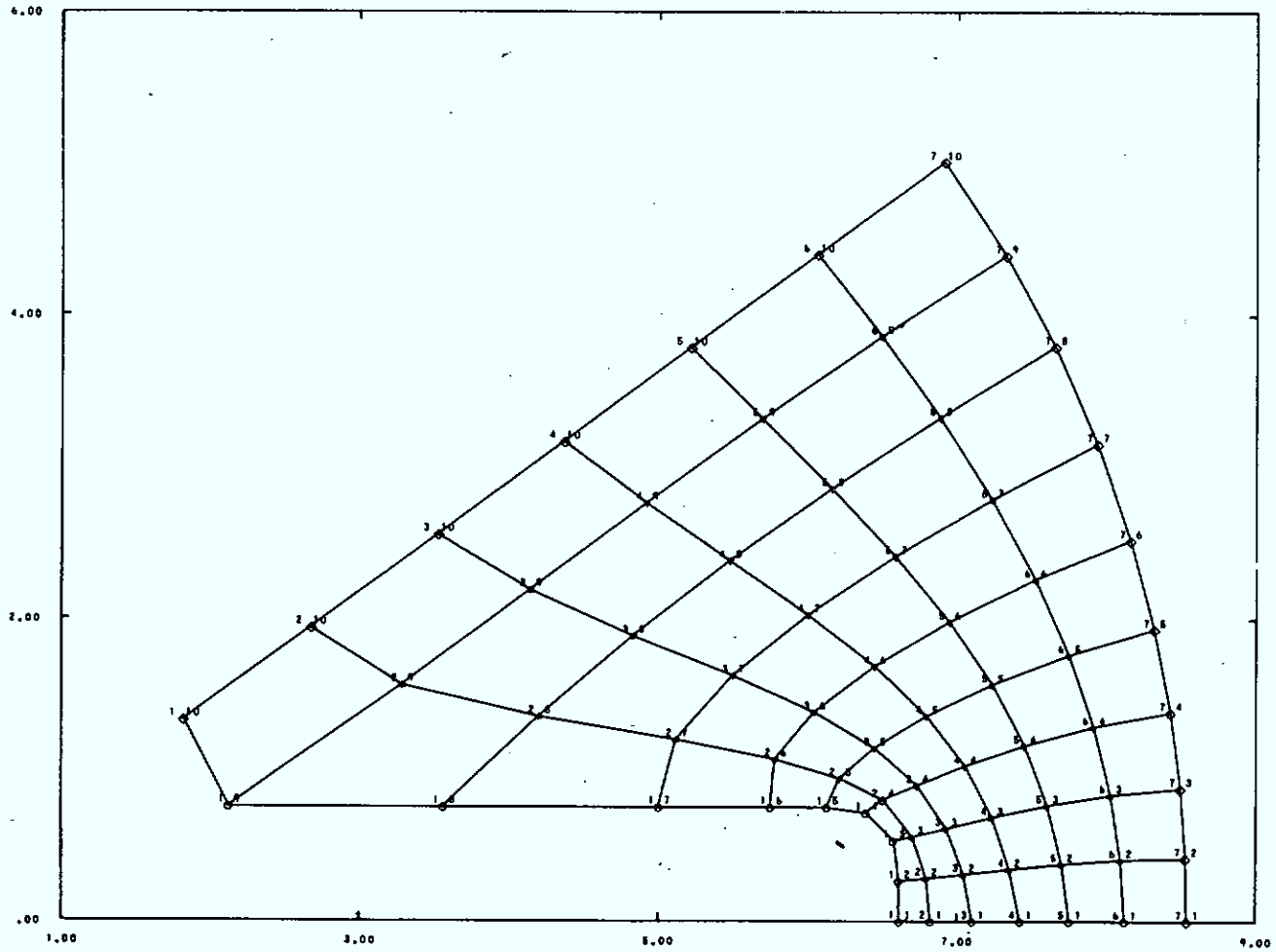

FIGURE 5a - Finite Element Model of the Booster Cavity Cross Section

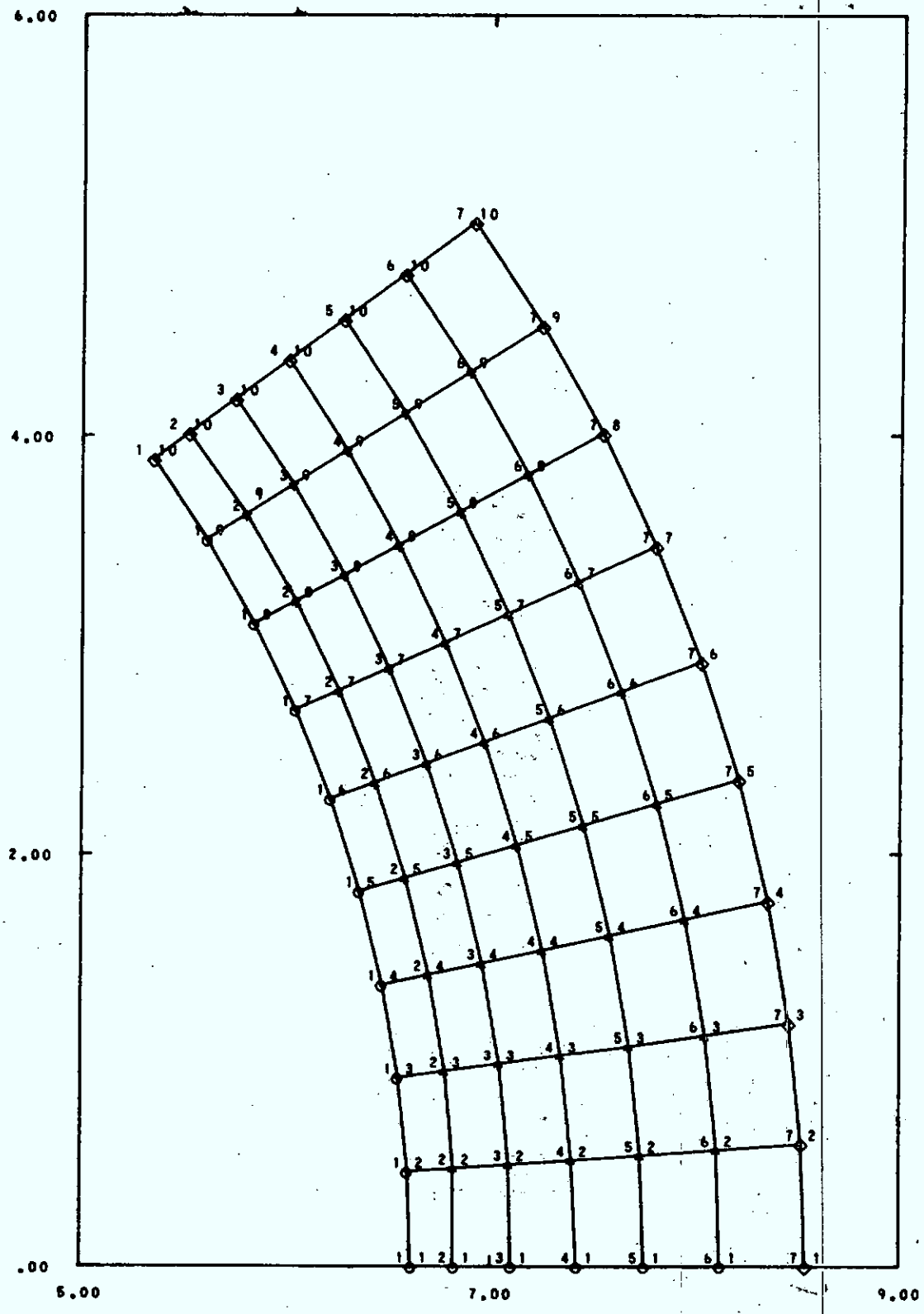

FIGURE 5b - Finite Element Model of the Axisymmetric Booster Cavity

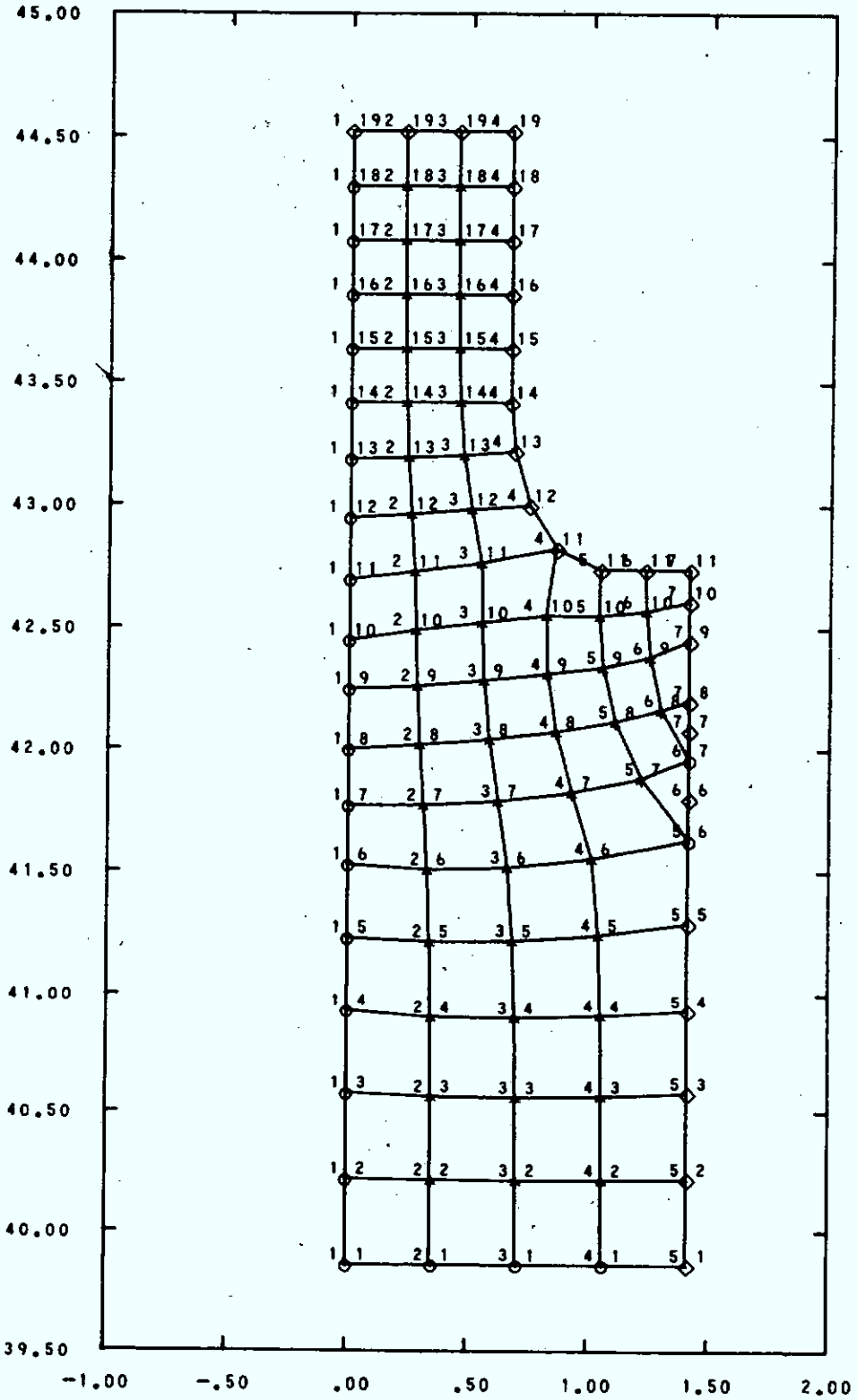

FIGURE 6 - Finite Element Model of the Finocyl Transition Region

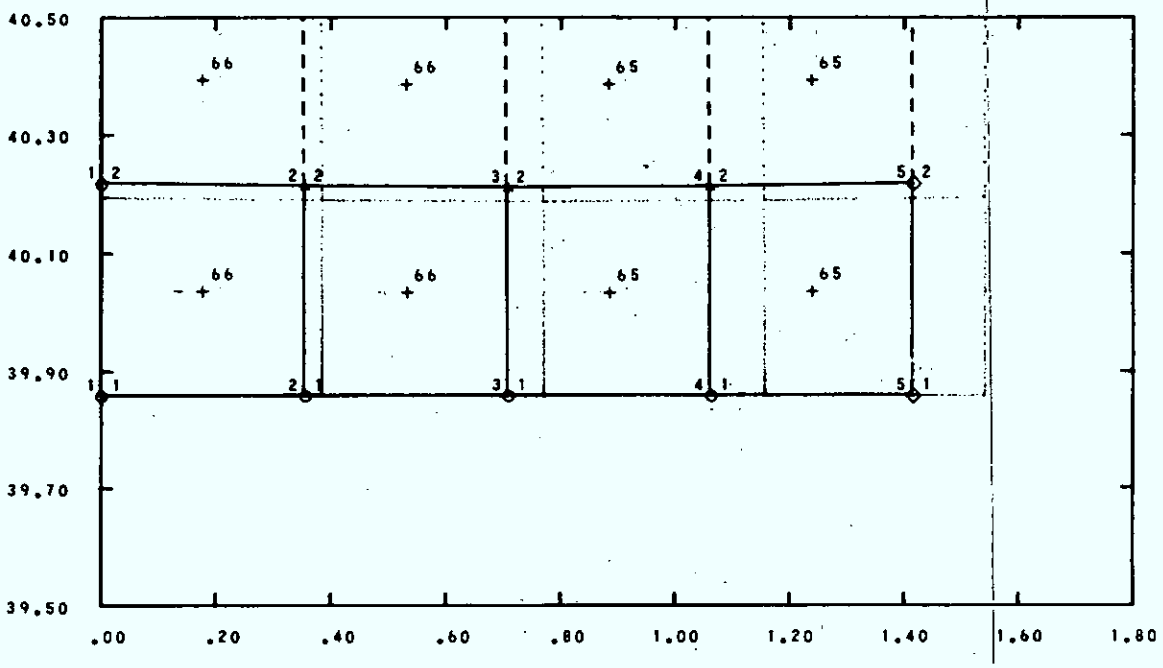

FIGURE 7a - Finocyl Transition Stresses/Displacements (2-3 in away from the Fin Tip)

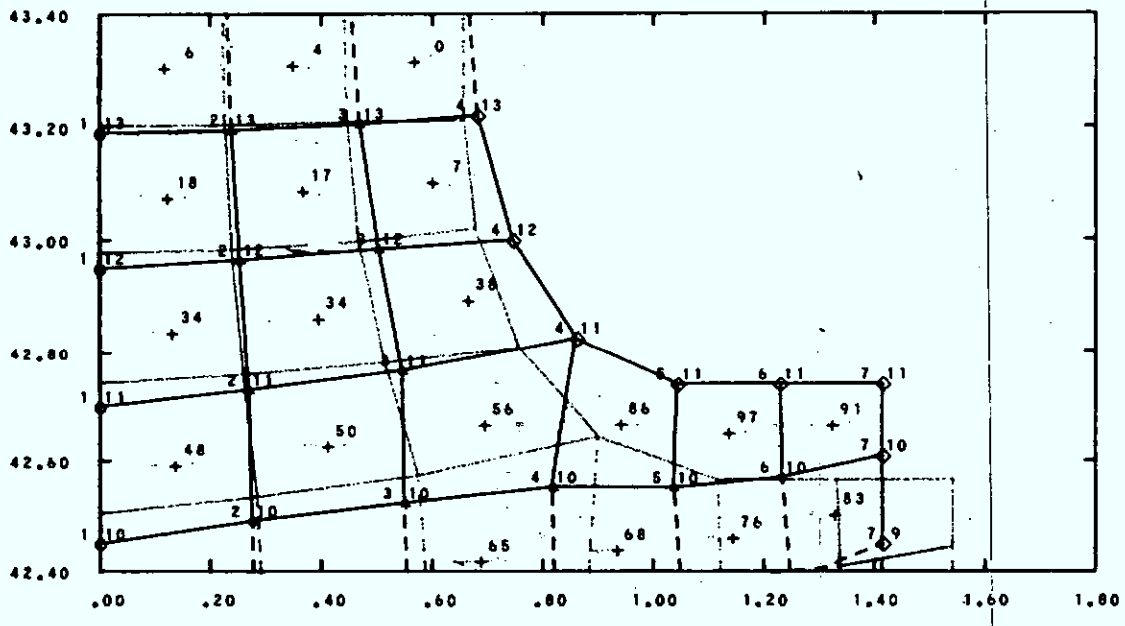

FIGURE 7b - Finocyl Transition Stresses/Displacements (at the Fin Tip)

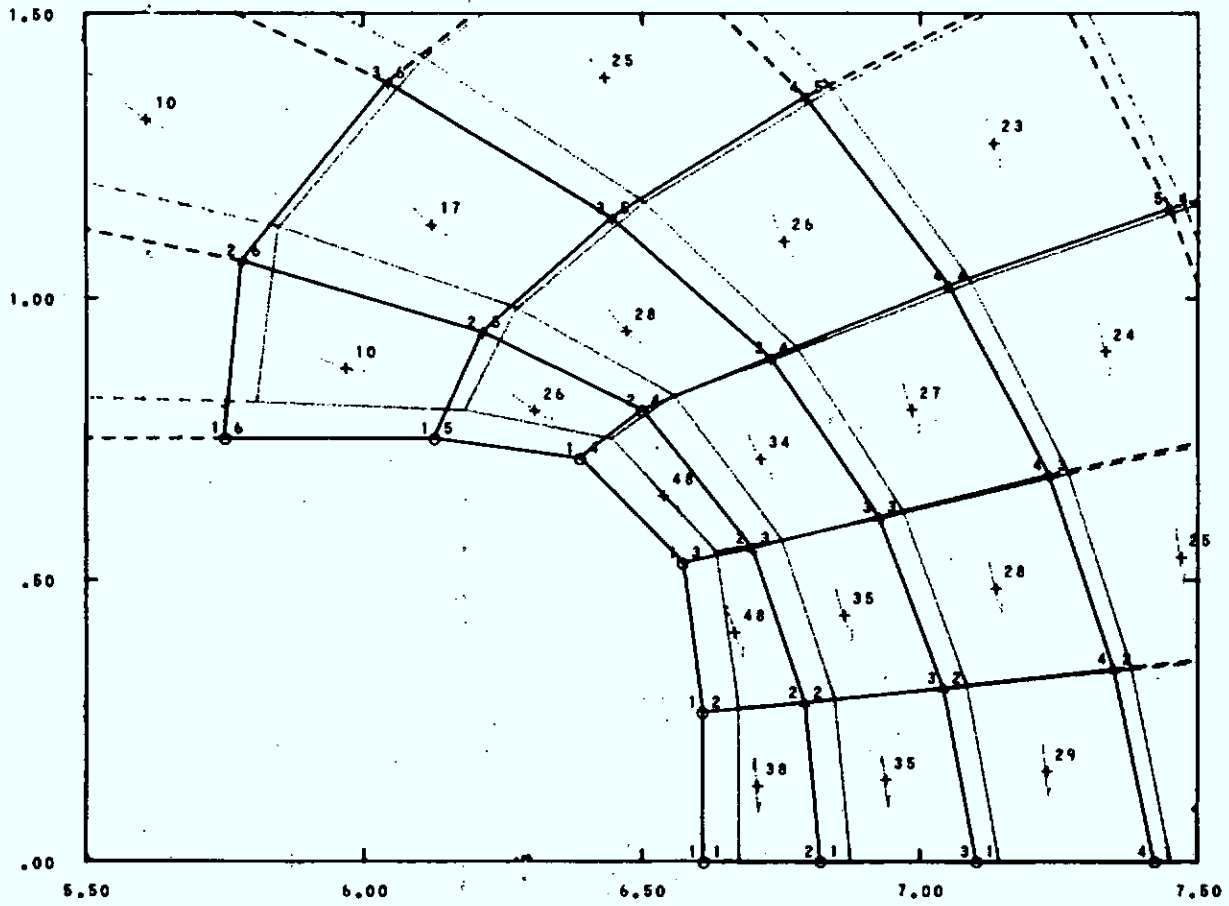

FIGURE 8a - Booster Cavity Cross Section: Stresses/Displacements (at the Fin Tip)

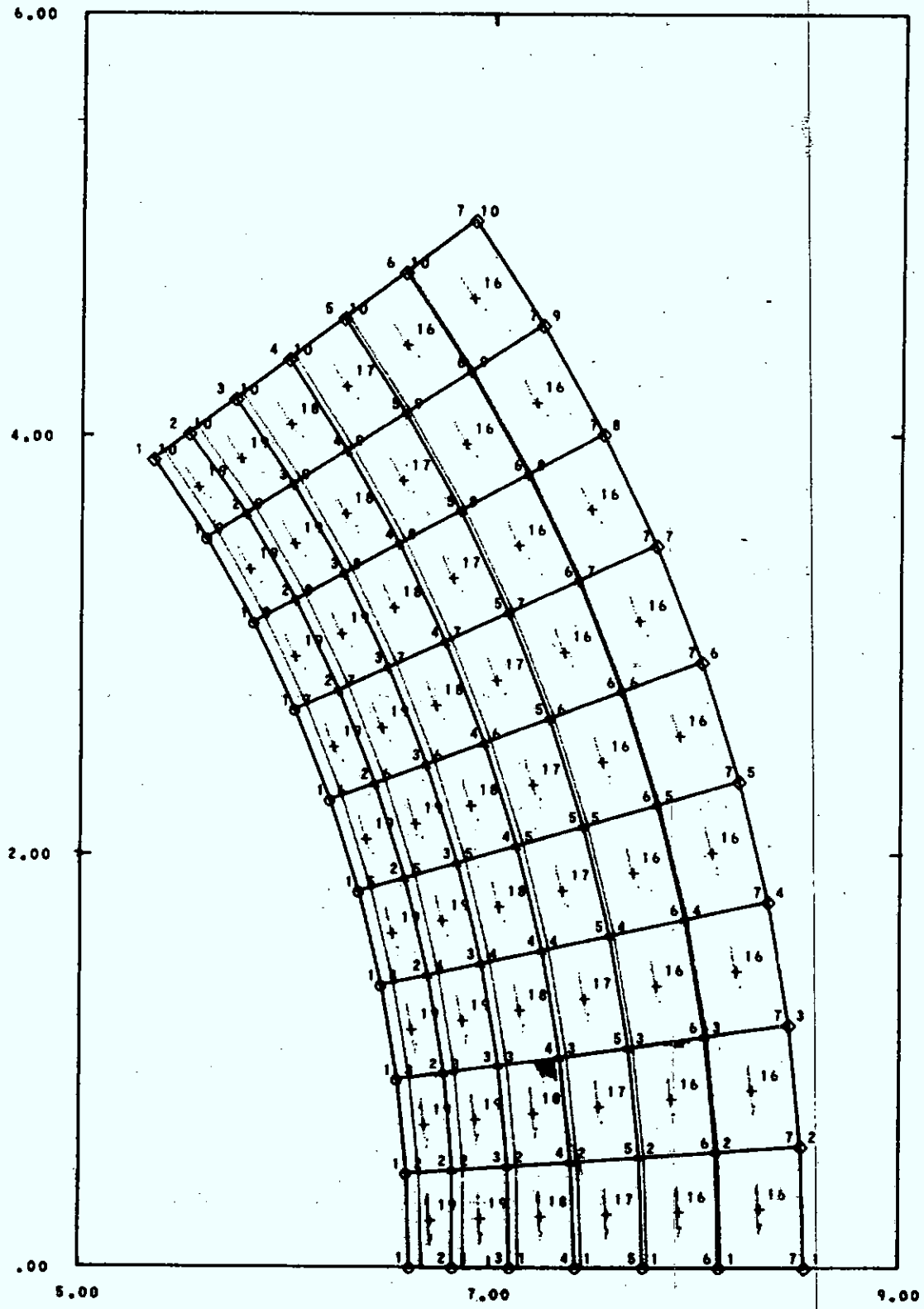

FIGURE 8b - Booster Cavity Axisymmetric Cross Section Stresses/Displacements

3) The main results of the axisymmetric analysis of the complete grain (Figs. 9a, b, c, d and e, and Appendix D) were the following:

a) when extrapolated to the surface, the inner bore hoop strain, approximately at the motor mid-length, was evaluated as

$$\varepsilon_{max}\ [5,17] = 0.0905 \qquad [13]$$

b) when extrapolated to the surface, the hoop strain at the finocyl transition was 0.079. With the appropriate SCF calculated in eq. 11, it became

$$\varepsilon_{max}\ [4,26] = 1.487 \times 0.079$$

$$= 0.117 \qquad [14]$$

c) after extrapolation, the hoop strain at the fin tip was computed as 0.0055. With the SCF calculated by eq. 12, the maximum strain was

$$\varepsilon_{max}\ [6,34] = 0.0055 \times 4.25$$

$$= 0.0234 \qquad [15]$$

Note: Extrapolated according to the equation

$$\varepsilon_0 = \varepsilon_1 \frac{(r_1)^2}{(r_0)^2}$$

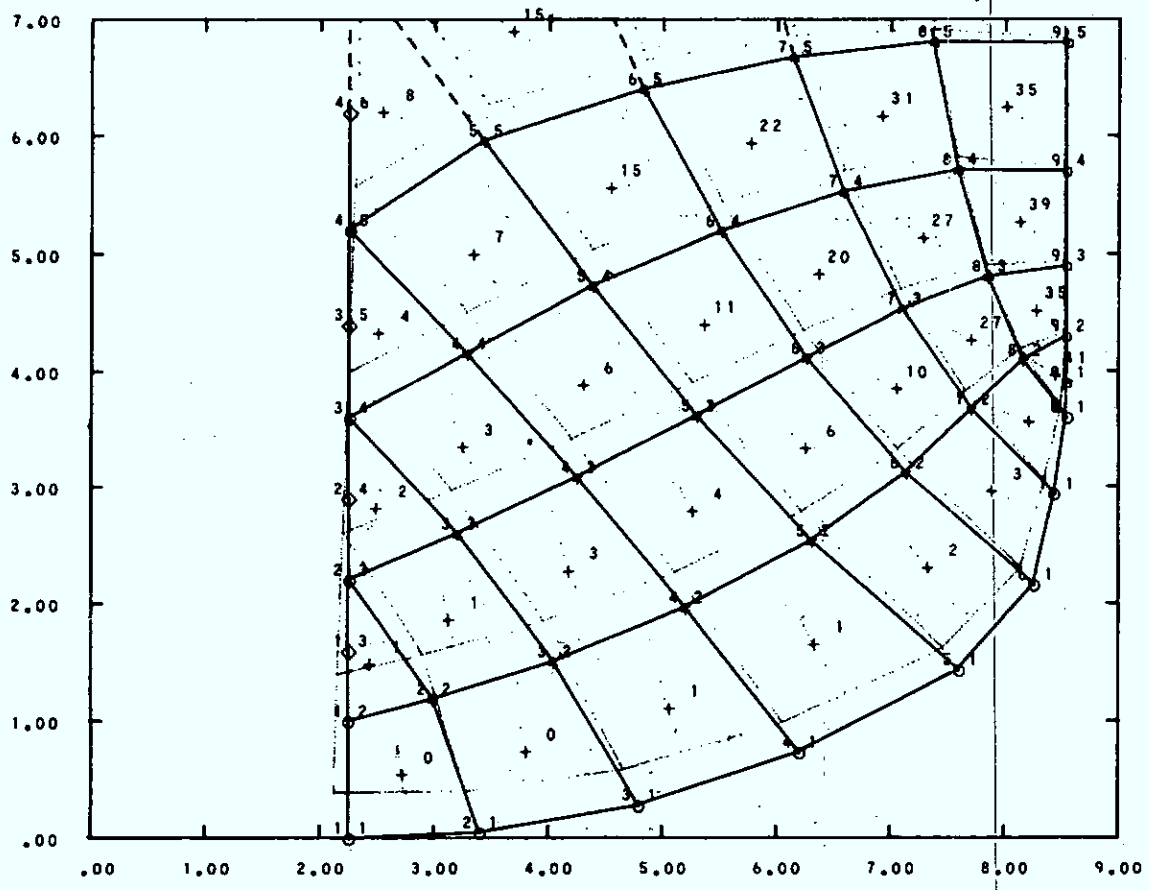

FIGURE 9a - Thermal Loading Stresses/Displacements: Motor Head-End

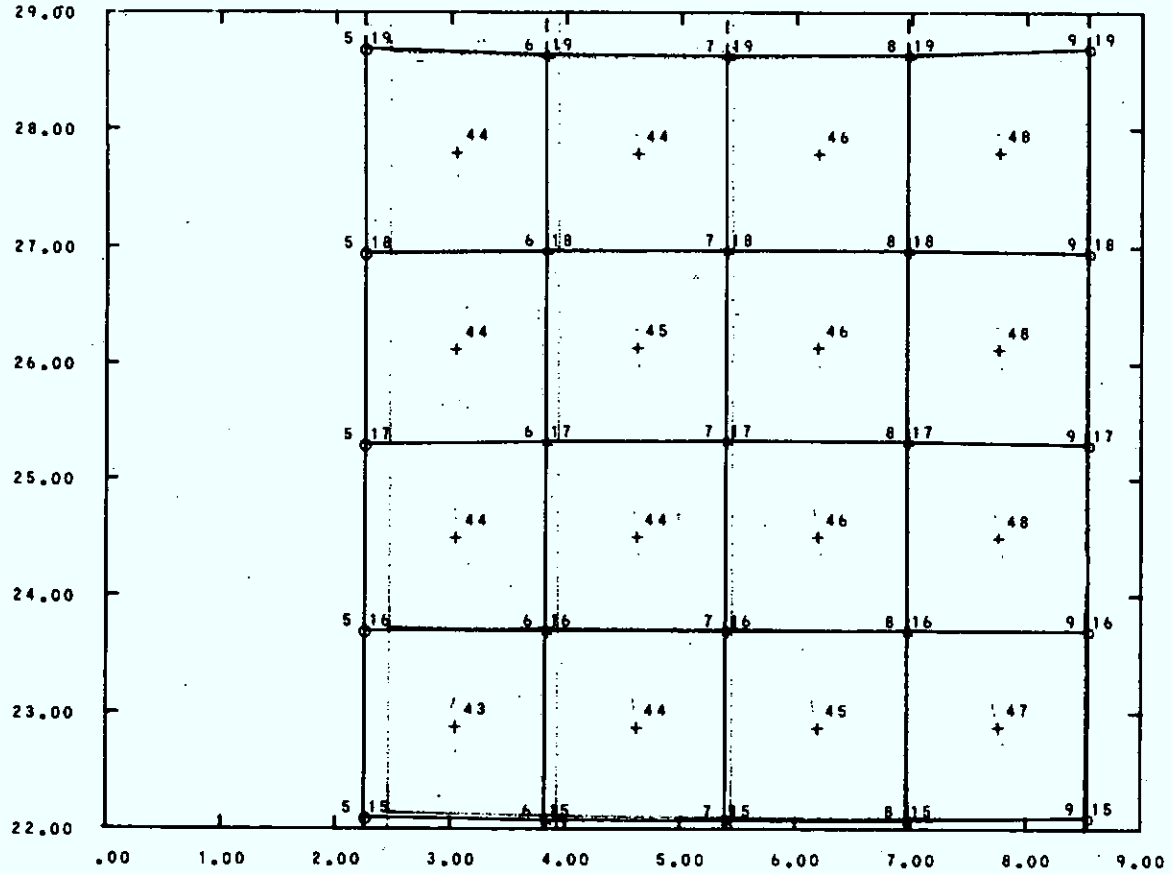

FIGURE 9b - Thermal Loading Stresses/Displacements: Motor Mid-Section

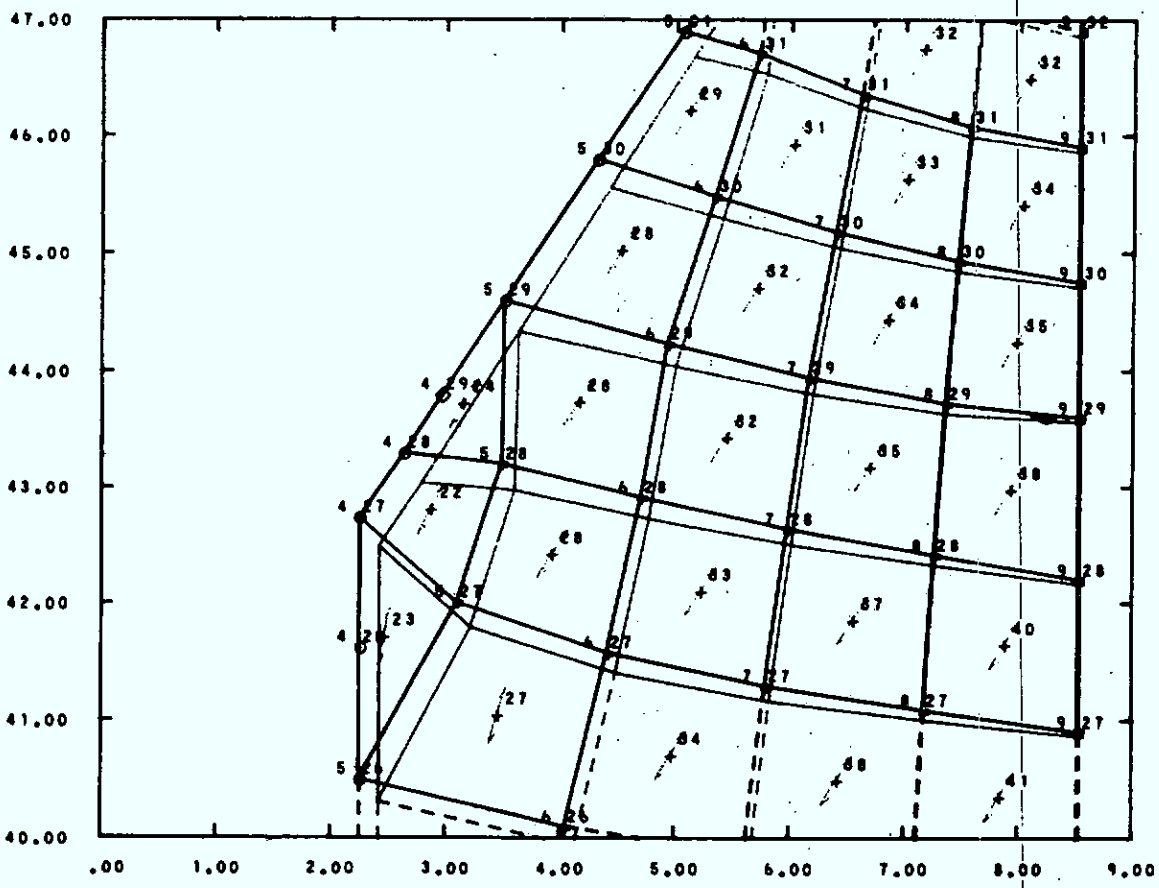

FIGURE 9c - Thermal Loading Stresses/Displacements: Finocyl Transition Region

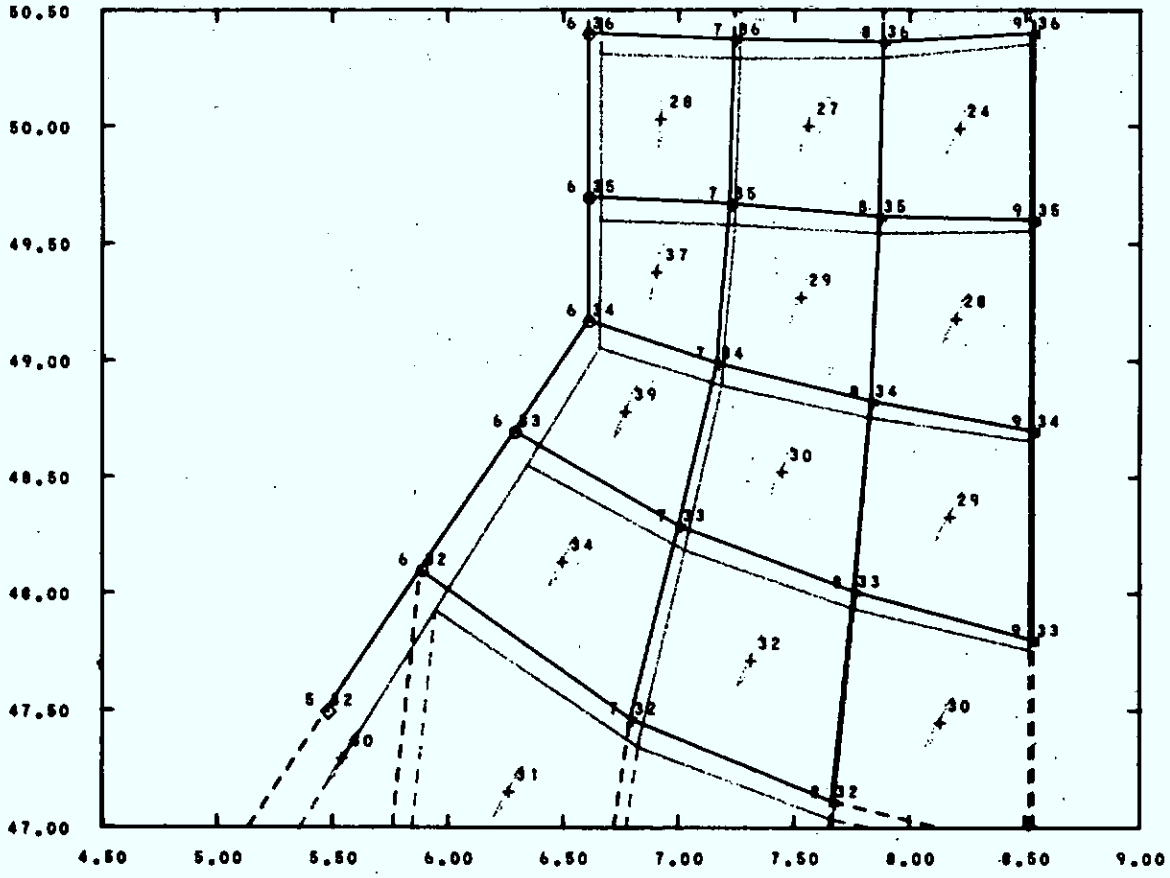

FIGURE 9d - Thermal Loading Stresses/Displacements: Booster Cavity Fin Tip

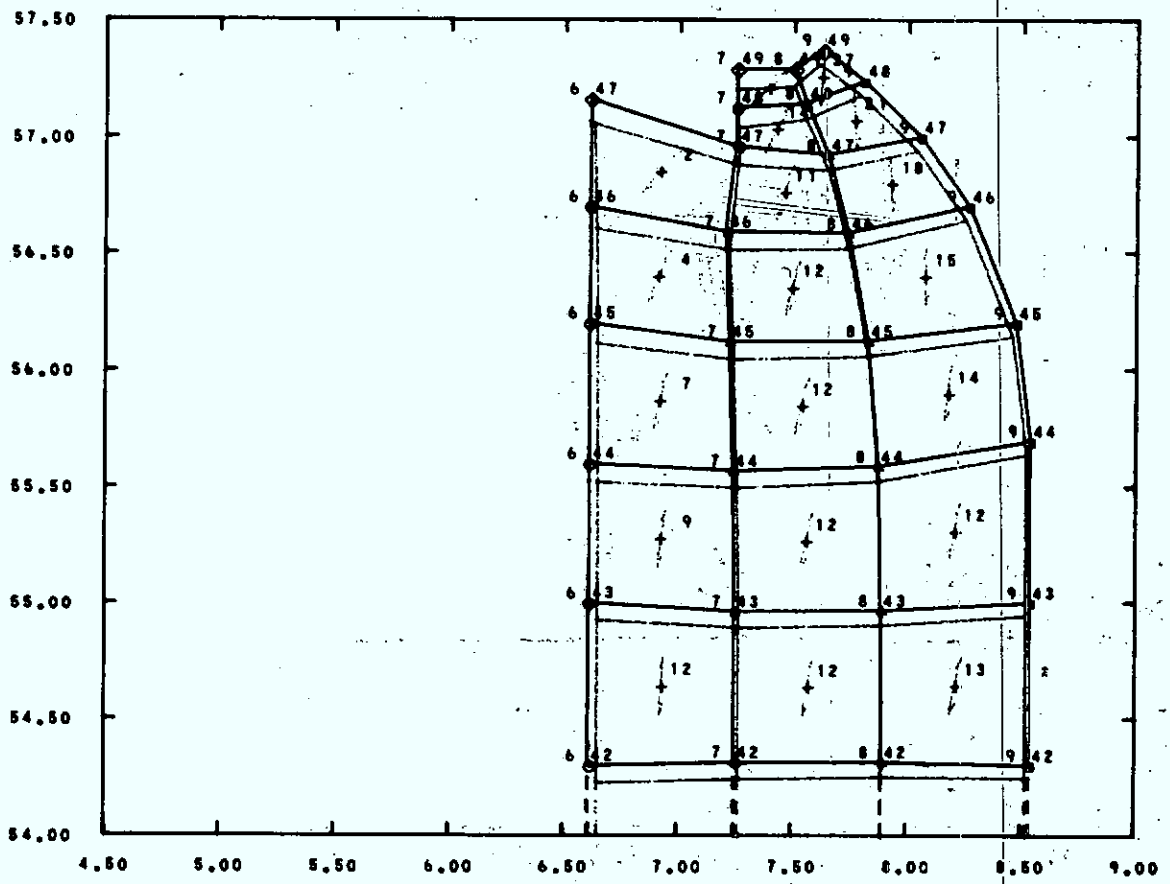

FIGURE 9e - Thermal Loading Stresses/Displacements: Motor Nozzle-End

d) the shear stress at the forward case-grain termination was

$$\tau_{r-z}\ [8,1] = 21.7 \text{ psi} \qquad [16]$$

e) the case-grain interfacial stress at the mid-length of the motor was estimated as

$$\sigma_r\ [8.17] = 41 \text{ psi} \qquad [17]$$

2.2 Acceleration Loading

2.2.1 General

During the ascent of a solid rocket vehicle, high shear stresses are normally induced at the forward termination point of the case and grain. It is particularly important here because the 17KS12000 is a third-stage motor left unpressurized during acceleration; pressurization would of course induce a hydrostatic compression field, thus enhancing the load carrying capability of the propellant. The axial deformation (or slump) is also worth being considered.

High-temperature acceleration is more severe than low-temperature acceleration because of the reduced bond strength capability and shear modulus.

2.2.2 Input data

1) The propellant mechanical properties were calculated as follows. Assuming that acceleration would last one minute, i.e. the combined burning times of the first and second stages,

and that the motor temperature at launch would be T = 110°F (316.3 K), a reduced time was calculated, using eqs. A-1 and A-3:

$$\log \frac{t}{a_T} = \log t - \log a_T \qquad [A\text{-}1]$$

$$= \log 1 - \left[\frac{-8.86(316.3-239)}{316.3-137.4} + 3.18 \right]$$

$$= 0.65 \qquad [18]$$

At that reduced time, it was possible to infer from Figs. 1, 2, and 3

$$E = 353 \text{ psi} \qquad [19]$$

$$\varepsilon_m = 0.205 \qquad [20]$$

$$\sigma_m = 73.5 \text{ psi} \qquad [21]$$

2) With the specified axial acceleration (15 g_n) and the propellant specific weight, 0.0647 lb_m/in^3 (Table I), a body force BFZ of 0.0647 x 15 = 0.9705 lb_f/in^3 was input as one of the propellant physical properties.

3) The payload weight was assumed to be 450 lb_m. A body force of 450 x 15 = 6750 lb_f was thus applied at node 9,1, the assumed payload/motor junction. Node 9,44 was considered as the attachment point of the motor to the second stage.

4) Since the specific weight of steel is 0.283 lb_m/in^3 (Table I), a body force BFZC of 0.283 x 15 = 4.25 lb_f/in^3 was input as one of the casing material properties.

2.2.3 Computer Analysis

A single longitudinal, axisymmetric, finite element analysis (AMGO 32) was performed with the model previously used for the thermal loading stress analysis (Fig. 4), but applying the appropriate data calculated above.

Pertinent pages of the computer printouts are included as Appendix E; Figs. 10a and b illustrate the main results.

2.2.4 Results

1) The shear stress at the forward case-grain termination was computed as

$$\tau_{r-z}\ [8.1] = 5.0 \text{ psi} \qquad [22]$$

2) The axial slump, which is maximum at the forward end of the inner bore node, 1,1, was

$$\Delta z\ (1,1) \approx 0.120 \text{ in} \qquad [23]$$

2.3 Pressurization Loading

2.3.1 General

The ignition pressurization induces a compressive hydrostatic stress throughout the grain with a superimposed tensile hoop stress and strain at the inner bore.

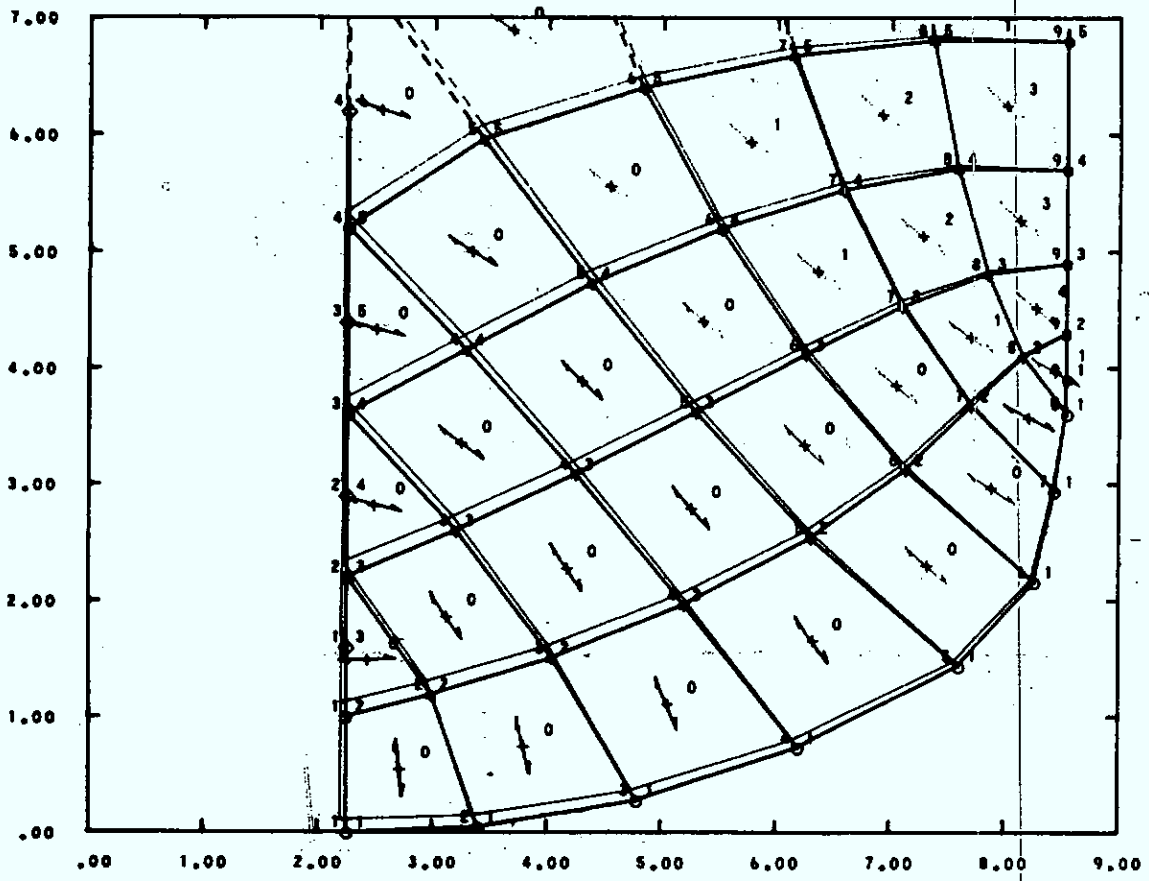

FIGURE 10a - Acceleration Loading Stresses/Displacements: Motor Head-End

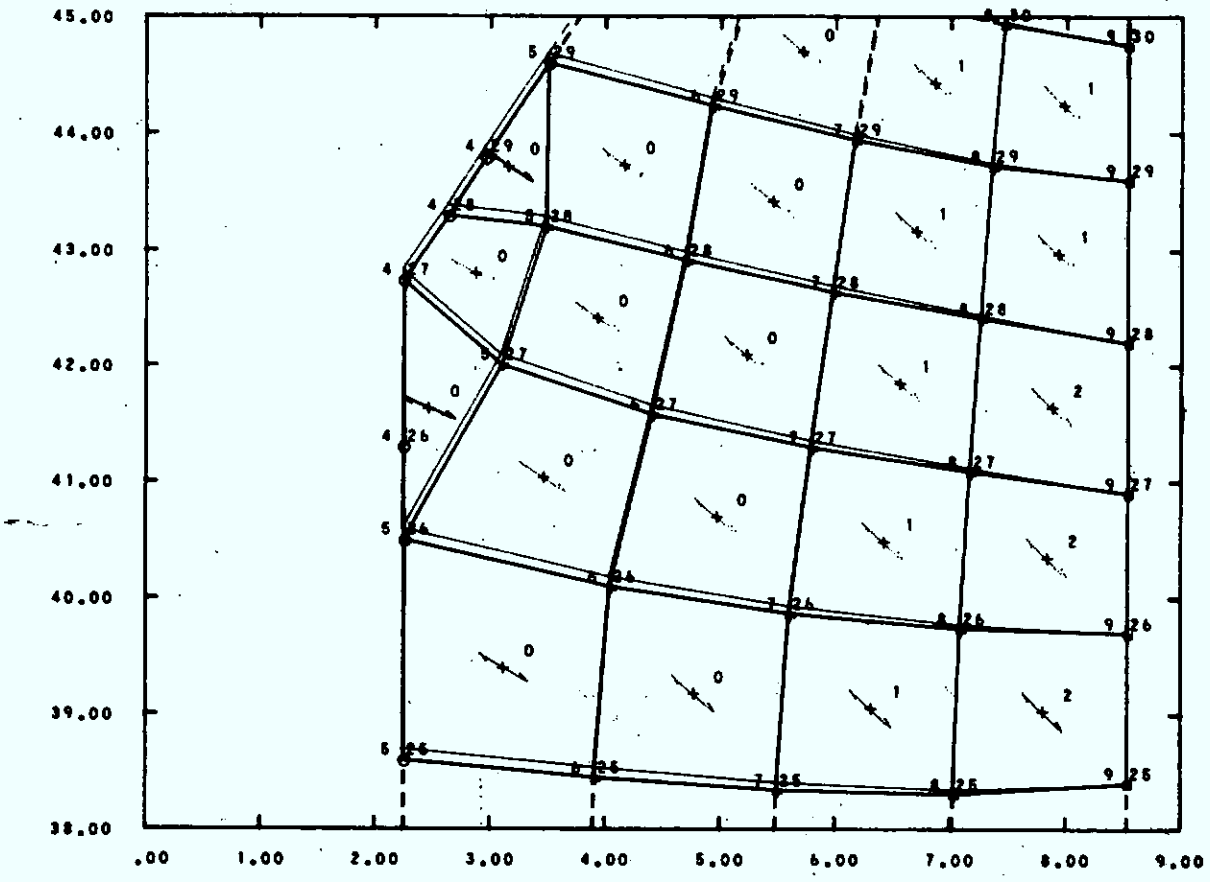

FIGURE 10b - Acceleration Loading Stresses/Displacements: Finocyl Transition Region

The hoop strain at the inner bore and the stresses at the termination points of the grain were considered critical. The analysis was based on the mechanical properties determined at low temperature ($-10^{o}F$).

2.3.2 Input data

1) Assuming an ignition pressure rise time of 100 ms (1.67×10^{-3} min) at T = $10^{o}F$ (250 K) a reduced time was calculated from eqs. A-1 and A-3

$$\log \frac{t}{a_T} = \log t - \log a_T \qquad [A\text{-}1]$$

$$= \log 1.67 \times 10^{-3} - \left[\frac{-8.86(250-239)}{250-137.4} + 3.18\right]$$

$$= -5.09 \qquad [24]$$

With that reduced time, Figs. 1, 2 and 3 show the following mechanical properties for the propellant:

$$E = 7330 \text{ psi} \qquad [25]$$

$$\varepsilon_m = 0.40 \qquad [26]$$

$$\sigma_m = 284.5 \text{ psi} \qquad [27]$$

2) It was (conservatively) assumed that the ignition pressure (1 000 psi) would induce an axial force of $1\,000 \times \Pi \times (8.537)^2 = 229\,000$ lb_f in the casing. That was input at node 9,1.

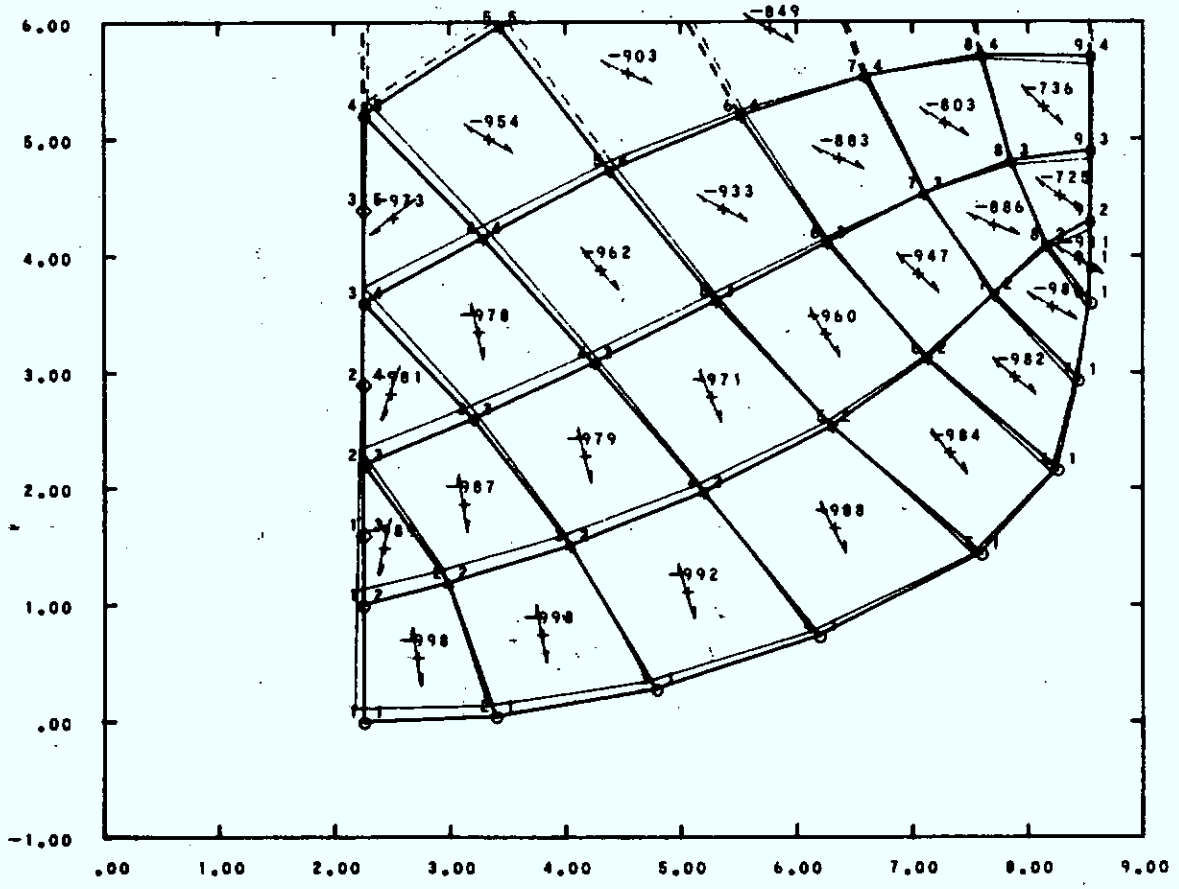

FIGURE 11a - Pressurization Loading Stresses/Displacements: Motor Head-End

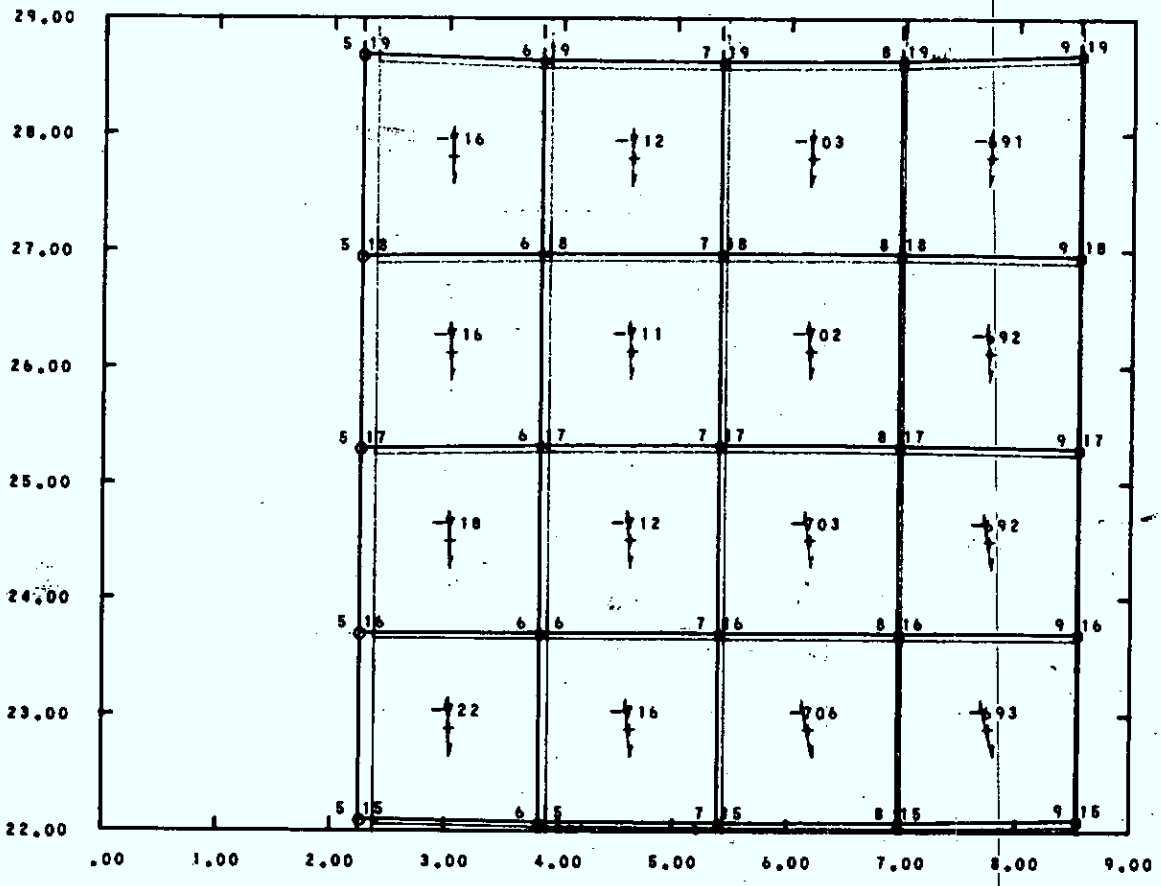

FIGURE 11b - Pressurization Loading Stresses/Displacements: Motor Mid-Plane

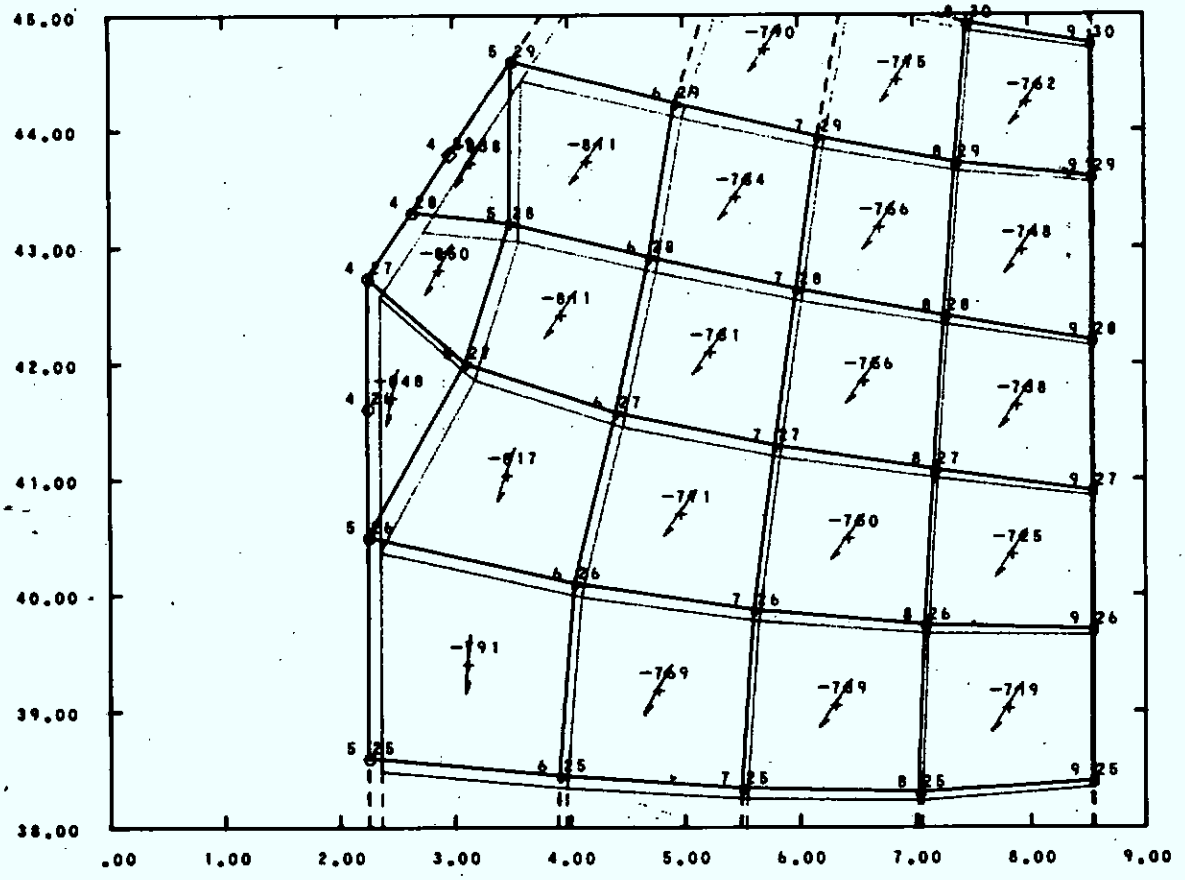

FIGURE 11c - Pressurization Loading Stresses/Displacements: Finocyl Transition Region

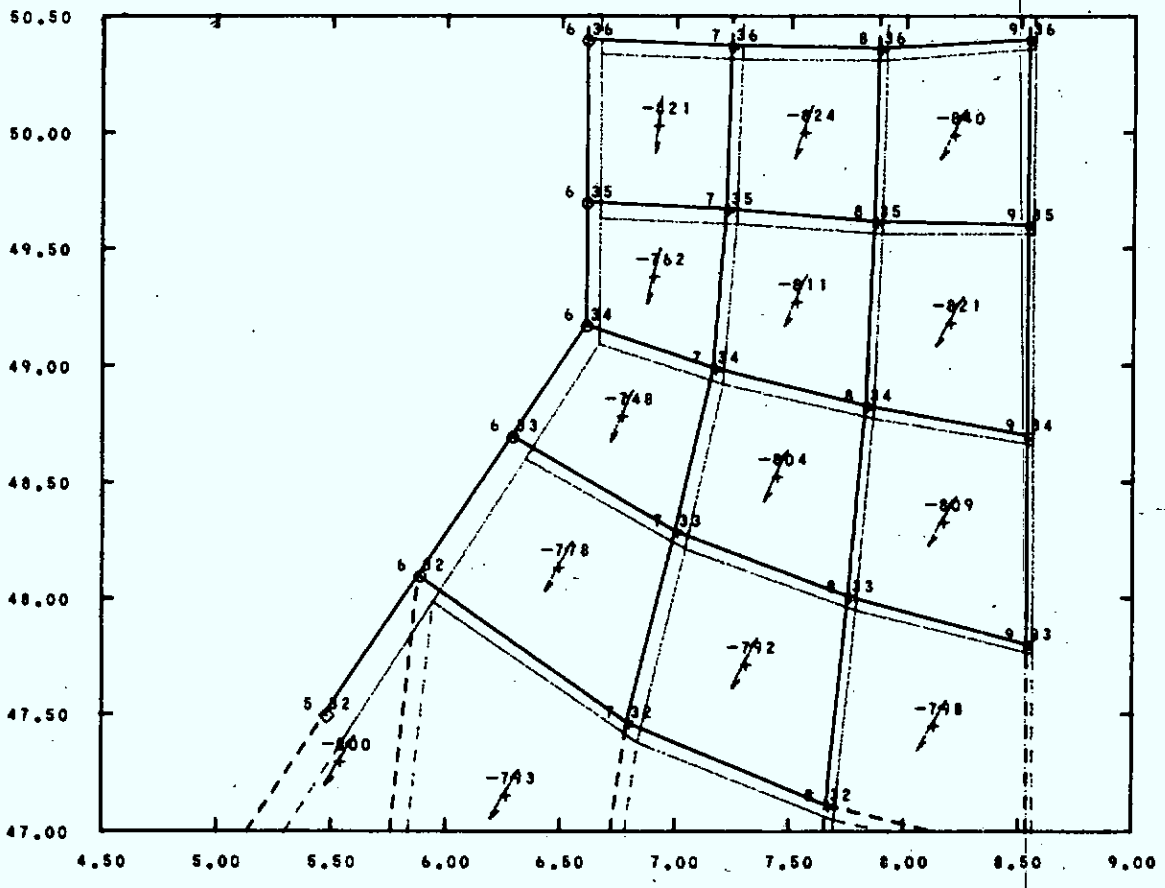

FIGURE 11d - Pressurization Loading Stresses/Displacements: Booster Cavity Fin Tip

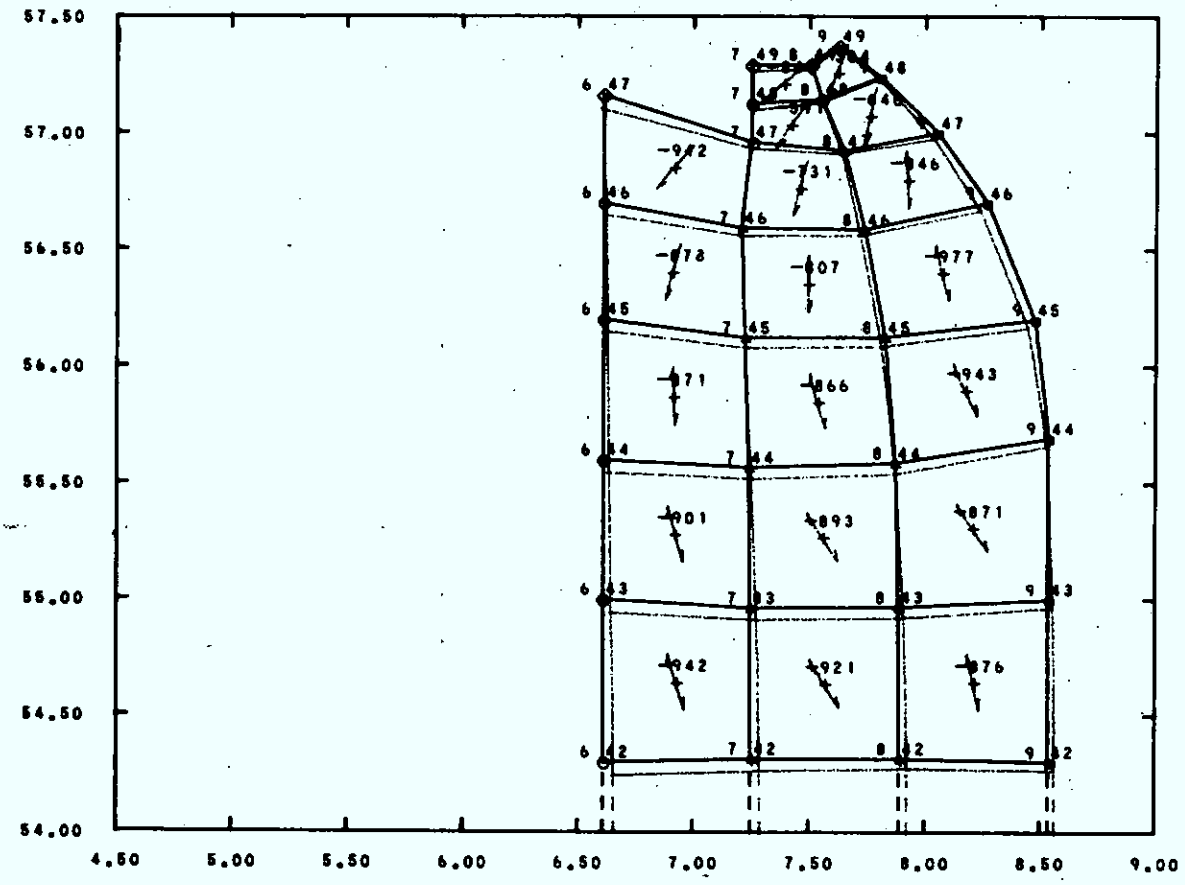

FIGURE 11e - Pressurization Loading Stresses/Displacements: Motor Nozzle-End

2.3.3 Computer Analysis

Applying the data calculated above to the model previously used for the thermal loading structural analysis, we performed an axisymmetric finite element analysis (AMGO 32).

The strain concentration factors computed for the structural analysis of the thermal loading were applied, as required.

Pertinent pages from the computer outputs are included in Appendix F; Figs. 11a, b, c, d, and e illustrate the main results.

2.3.4 Results

1) After an appropriate extrapolation to the surface, the inner bore hoop strain at the mid-length of the motor was computed as

$$\varepsilon_{max}\ [5,17] = 0.00584 \qquad [28]$$

2) When extrapolated to the surface, the hoop strain at the finocyl transition was calculated as 0.0514. With the SCF of eq. 11, it became

$$\varepsilon_{max}\ [4,26] = 1.487 \times 0.0514$$

$$= 0.0764 \qquad [29]$$

3) After extrapolation to the surface, the calculated hoop strain at the fin tip was 0.0080. With the appropriate SCF of eq. 12, it became

$$\varepsilon_{max}\ [6,34] = 4.25 \times 0.0080$$

$$= 0.0340 \qquad [30]$$

4) The maximum shear stress at the forward termination of the case-grain was calculated as

$$\tau_{r-z}\ [8,1] = 132.3 \text{ psi} \qquad [31]$$

3.0 FAILURE ANALYSES

3.1 General

Because of the various unknowns associated with the structural analyses, specifically with the propellant behavior and the failure criteria, a minimum safety factor (SF) of 2.0 is desirable; it is usually based on the mean properties of an unaged propellant minus 3σ. When the statistical properties of the propellant are not available, it may be conservatively considered that 1σ = 10% of the relevant property (Ref. 1).

3.2 Thermal Loading

1) Under the stated conditions, the lower limit of the maximum strain capability was $\varepsilon_m = 0.20$ (eq. 9). The maximum strain calculated at the finocyl transition region was 0.117 (eq. 14). Therefore, the strain-based safety factor is

$$SF = \frac{0.20}{0.117} = 1.71 \qquad [32]$$

2) The shear stress at the forward case-grain termination was calculated as 21.7 psi (eq. 16). The maximum allowable shear stress is usually considered to be 70% of the uniaxial tension failure stress (Ref. 1). Since σ_m = 54.5 psi (eq. 10),

$$\tau_m = 0.70 \times 54.5 = 38.2 \text{ psi} \qquad [33]$$

and the

$$SF = \frac{38.2}{21.7} = 1.76 \qquad [34]$$

3.3 Acceleration Loading

1) The maximum shear stress expected was calculated as 5.0 psi (eq. 22). Using eq. 33, since σ_m = 33.5 (eq. 21), the maximum admissible shear stress is

$$\tau_m = 0.70 \times 73.5$$

$$= 51.5 \text{ psi} \qquad [35]$$

Therefore, the

$$SF = \frac{51.5}{5.0} = 10.3 \qquad [36]$$

2) The maximum slump calculated, 0.120 in, (eq. 23) is deemed acceptable.

3.4 Pressurization Loading

a. It is generally accepted that pressurized biaxial tests, used to evaluate port cracking during ignition pressurization, yield a maximum tensile strain 2.5 times higher than the standard uniaxial test. Thus, from eq. 26,

$$\varepsilon_{max}^{2\text{-}D} = 2.5 \times 0.4 = 1.0 \qquad [37]$$

Since the maximum induced strain has been evaluated as 0.0764 (eq. 29), it follows that

$$SF = \frac{1.0}{0.0764} = 13.1 \qquad [38]$$

b. The maximum shear stress calculated at the forward termination of the case-grain was 132.3 psi (eq. 31). Since the maximum admissible shear stress can be estimated as

$$\tau_m = 0.70 \times (\sigma_m = 284.5) = 199.2 \text{ psi} \qquad [39]$$

(eqs. 33 and 27), then

$$SF = \frac{199.2}{132.3} = 1.51 \qquad [40]$$

4.0 DISCUSSIONS

It is generally agreed throughout the rocket industry that strain-based safety factors are the best acceptance criteria; indeed, for viscoelastic materials, strains and displacements are usually more exactly predicted than stresses (Ref. 1). Therefore, only strain-based SF will be considered critical herein.

The minimum strain-based SF computed is 1.71 (eq. 32) under conditions of thermal loading. This is somewhat lower then the generally recommended SF, but it is sufficiently close to 2.0 that no problem is anticipated, when the rationale behind such an acceptable SF (see para. 3.1) is understood.

In regard to the minimum stress-based SF of 1.51, calculated for the pressurization loading analysis, it is somewhat low but not considered critical because of the conservative assumption made regarding the input data. Indeed, by merely choosing the lower limit of the modulus, instead of the upper limit, we would obtain a SF of approximately 4.0, instead of 1.51, indicating that the actual SF is likely around 2.7; this is considered more realistic and more acceptable.

5.0 CONCLUSIONS

Since the estimated strain-based safety factor is 1.71, the modified 17KS12000 motor grain appears structurally adequate for the three load cases considered (thermal, acceleration, and pressurization loadings).

6.0 REFERENCES

1. Fitzgerald, J.E. and Hufferd, W.L., "Handbook for the Engineering Structural Analysis of Solid Propellants", Chemical Propulsion Information Agency, Silver Springs, Md., May 1971. (CPIA Pub. No. 214) UNCLASSIFIED

2. Williams, M.L, Landel, R.F. and Ferry, J.D. "The Temperature Dependence of Relaxation Mechanisms in Amorphous Polymers and other Glass-forming Liquids". J.Am. Chem. Soc., Vol. 77, p. 3701-3707, 1955.

3. Becker, E.B., and Brisbane, J.J. "Application of the Finite Element Method to Stress Analysis of Solid Propellant Rocket Grains". Rohm & Haas Ltd., Special Report S-76, Vol. 1 & 2, Nov. 1965. UNCLASSIFIED

APPENDIX A

WLF Reduced Variables Equations

1. Reduced Time

$$\log \frac{t}{a_T} \qquad [A\text{-}1]$$

with

t: duration of application of the load (in minutes). For constant strain-rate testing

$$t = \frac{GL}{R} \varepsilon_m \qquad [A\text{-}2]$$

with GL = 3.32 in

$$\log a_T = \frac{-8.86(T-239)}{T-137\ 4} + 3.18 \qquad [A\text{-}3]$$

2. Reduced Modulus

$$\log \frac{E\ 297}{T} \qquad [A\text{-}4]$$

3. Reduced Stress

$$\log \sigma_m \lambda_m \frac{297}{T} \qquad [A\text{-}5]$$

APPENDIX B

17KS12000

Finocyl Transition Region

Structural Analysis

Computer Printouts

I J/ ANGLE	COORDINATES X	Y	STRESS / STRAIN X	Y	AXIAL Z	SHEAR X-Y	MAXIMUM	MINIMUM	MAX SHEAR
1 1	.176	40.039	6.6337E 01	-3.7035E-01	7.4345E-16	4.4427E-02	6.6337E 01	-3.7038E-01	3.3384E 01
.04	1.6359E-01		9.1245E-02	-6.4406E-02	-6.3542E-02	2.0733E-04	9.1245E-02	-6.4407E-02	1.5565E-01
2 1	.529	40.037	6.6174E 01	-1.5410E-01	7.4346E-16	1.0719E-01	6.6174E 01	-1.5427E-01	3.3164E 01
.09	1.6371E-01		9.0823E-02	-6.3942E-02	-6.3883E-02	8.0024E-04	9.0823E-02	-6.3943E-02	1.5477E-01
3 1	.883	40.037	6.5943E 01	1.5351E-01	7.4345E-16	1.0647E-01	6.5943E 01	1.5334E-01	3.2895E 01
.09	1.6390E-01		9.0224E-02	-6.3284E-02	-6.3642E-02	4.9688E-04	9.0225E-02	-6.3285E-02	1.5351E-01
4 1	1.237	40.039	6.5781E 01	3.6921E-01	7.4346E-16	4.3872E-02	6.5781E 01	3.6918E-01	3.2706E 01
.04	1.6402E-01		8.9805E-02	-6.2822E-02	-6.3684E-02	2.0474E-04	8.9805E-02	-6.2822E-02	1.5263E-01
1 2	.176	40.395	6.6446E 01	-5.5154E-01	7.4345E-16	1.5021E-01	6.6446E 01	-5.5187E-01	3.3498E 01
.13	1.6342E-01		9.1553E-02	-6.4772E-02	-6.3486E-02	7.0098E-04	9.1554E-02	-6.4772E-02	1.5633E-01
2 2	.527	40.388	6.6217E 01	-2.8851E-01	-5.8042E-16	3.8996E-01	6.6219E 01	-2.3046E-01	3.3285E 01
.31	1.6364E-01		9.0948E-02	-6.4092E-02	-6.3589E-02	1.6798E-03	9.0952E-02	-6.4097E-02	1.5506E-01
3 2	.881	40.388	6.5902E 01	2.2504E-01	7.4345E-16	3.8833E-01	6.5904E 01	2.2308E-01	3.2840E 01
.31	1.6397E-01		9.0104E-02	-6.3141E-02	-6.3666E-02	1.6722E-03	9.0109E-02	-6.3146E-02	1.5386E-01
4 2	1.236	40.395	6.5677E 01	8.4600E-01	7.4346E-16	1.4878E-01	6.5678E 01	8.4566E-01	3.2566E 01
.13	1.6419E-01		8.9507E-02	-6.2466E-02	-6.3740E-02	6.9432E-04	8.9508E-02	-6.2467E-02	1.5197E-01
1 3	.174	40.744	6.6661E 01	-9.7227E-01	7.4345E-16	3.0375E-01	6.6662E 01	-9.7363E-01	3.3818E 01
.26	1.6293E-01		9.2216E-02	-6.8594E-02	-6.3326E-02	1.4175E-03	9.2219E-02	-6.5597E-02	1.5782E-01
2 3	.524	40.730	6.6312E 01	-4.0023E-01	7.4346E-16	7.2386E-01	6.6320E 01	-4.0809E-01	3.3364E 01
.62	1.6346E-01		9.1227E-02	-6.4434E-02	-6.3800E-02	3.3780E-03	9.1246E-02	-6.4458E-02	1.5570E-01
3 3	.877	40.733	6.5821E 01	3.8600E-01	7.4345E-16	7.3011E-01	6.5830E 01	3.7786E-01	3.2726E 01
.64	1.6416E-01		8.9854E-02	-6.2829E-02	-6.3730E-02	3.4072E-03	8.9872E-02	-6.2848E-02	1.5272E-01
4 3	1.234	40.746	6.5463E 01	9.8447E-01	7.4346E-16	3.0581E-01	6.5468E 01	9.8303E-01	3.2266E 01
.27	1.6465E-01		8.8888E-02	-6.1668E-02	-6.3889E-02	1.4243E-03	8.8861E-02	-6.1668E-02	1.5053E-01
1 4	.171	41.069	6.6958E 01	-1.6976E 00	7.4345E-16	5.0999E-01	6.6962E 01	-1.7014E 00	3.4332E 01
.43	1.6195E-01		9.3233E-02	-6.6963E-02	-6.3002E-02	2.3797E-03	9.3242E-02	-6.6972E-02	1.6021E-01

I J/ ANGLE	COORDINATES X	Y	STRESSES / STRAINS X	Y	AXIAL Z	SHEAR X-Y	MAXIMUM	MINIMUM	MAX SHEAR
3 9	.687	42.419	6.5641E 01	-8.9957E-01	7.4345E-16	1.1064E 00	6.5659E 01	-9.1797E-01	3.3288E 01
.98	1.6074E-01		9.0557E-02	-6.4703E-02	-6.2604E-02	5.1634E-03	9.0600E-02	-6.4746E-02	1.5535E-01
4 9	.932	42.440	6.8416E 01	6.0150E 00	7.4345E-16	6.4709E-02	6.8416E 01	6.0149E 00	3.1201E 01
.06	1.8308E-01		8.9678E-02	-8.5925E-02	-6.9960E-02	3.0197E-04	8.9678E-02	-8.5925E-02	1.4560E-01
5 9	1.143	42.461	7.6427E 01	8.9270E 00	7.4345E-16	-3.5065E 00	7.6608E 01	8.7454E 00	3.3932E 01
-2.97	2.0915E-01		9.9785E-02	-5.7714E-02	-7.8544E-02	-1.6364E-02	1.0021E-01	-8.8138E-02	1.5835E-01
6 9	1.327	42.503	8.3382E 01	6.0477E 00	7.4345E-16	-8.0161E 00	8.3438E 01	5.9952E 00	3.8720E 01
-1.49	2.1943E-01		1.1263E-01	-6.7818E-02	-8.1929E-02	-9.4084E-03	1.1275E-01	-6.7940E-02	1.8069E-01
1 10	.136	42.593	4.8941E 01	-7.0226E 00	.0000E 00	-1.5828E 00	4.8986E 01	-7.0674E 00	2.8027E 01
-1.62	1.0758E-01		6.9100E-02	-6.1483E-02	-4.5097E-02	7.3866E-03	6.9204E-02	-6.1587E-02	1.3079E-01
2 10	.409	42.628	5.0509E 01	-6.0735E 00	.0000E 00	-4.6483E 00	5.0888E 01	-6.4829E 00	2.8670E 01
-4.67	1.1330E-01		7.0873E-02	-6.1152E-02	-4.6980E-02	-2.1692E-02	7.1759E-02	-6.2037E-02	1.3380E-01
3 10	.693	42.667	5.5251E 01	-6.1226E-01	.0000E 00	-8.6445E 00	5.6558E 01	-1.9194E 00	2.9239E 01
-8.60	1.3601E-01		7.4459E-02	-5.5888E-02	-5.4459E-02	-4.0341E-02	7.7509E-02	-5.8938E-02	1.3645E-01
4 10	.939	42.668	8.3387E 01	1.0619E 01	7.4345E-16	-1.8193E 01	8.6431E 01	7.5748E 00	3.9488E 01
-11.33	2.2775E-01		1.0990E-01	-5.9892E-02	-8.4671E-02	-7.0898E-02	1.1700E-01	-6.6996E-02	1.8400E-01
5 10	1.135	42.651	9.6752E 01	6.6188E 00	7.4345E-16	-9.0060E 00	9.7643E 01	5.7277E 00	4.5958E 01
-5.65	2.5047E-01		1.3360E-01	-7.6707E-02	-9.2151E-02	-4.2028E-02	1.3566E-01	-7.8786E-02	2.1447E-01
6 10	1.322	42.666	9.1175E 01	1.3025E 00	7.4345E-16	-1.9097E 00	9.1216E 01	1.2619E 00	4.4977E 01
-1.22	2.2555E-01		1.2880E-01	-8.0908E-02	-8.3947E-02	-8.9118E-03	1.2889E-01	-8.1002E-02	2.0989E-01
1 11	.130	42.836	3.4078E 01	-3.2062E 00	.0000E 00	-2.8588E 00	3.4253E 01	-3.3810E 00	1.8817E 01
-3.91	8.2072E-02		4.2819E-02	-4.4178E-02	-3.6697E-02	-1.1941E-02	4.3227E-02	-4.4586E-02	8.7813E-02
2 11	.392	42.861	3.3014E 01	-3.4263E 00	.0000E 00	-7.8644E 00	3.4639E 01	-5.0511E 00	1.9848E 01
-11.67	7.9487E-02		4.1188E-02	-4.3840E-02	-3.5846E-02	-8.6700E-02	4.4979E-02	-4.7632E-02	9.2610E-02
3 11	.663	42.894	3.1768E 01	3.7499E 00	.0000E 00	-1.4767E 01	3.8114E 01	-2.5958E 00	2.0355E 01
-23.25	9.3242E-02		3.3750E-02	-3.1625E-02	-4.0375E-02	-6.8912E-02	4.8557E-02	-4.6432E-02	9.4989E-02

APPENDIX C-1

17KS12000

Booster Cavity Structural Analysis

Computer Printouts

I J/ ANGLE	COORDINATES X	Y	STRESSES / STRAINS X	Y	AXIAL Z	SHEAR X-Y	MAXIMUM	MINIMUM	MAX SHEAR
1 1	6.708	.138	9.1973E-01	3.8062E 01	2.5361E 01	-2.4887E 00	3.8228E 01	7.5371E-01	1.8737E 01
-86.18	1.0082E-01		-5.7028E-02	2.9636E-02	.0000E 00	-1.1614E-02	3.0023E-02	-5.7416E-02	8.7439E-02
2 1	6.938	.148	7.3074E 00	3.6027E 01	2.6895E 01	-3.1845E 00	3.6389E 01	6.9462E 00	1.4281E 01
-83.69	1.0812E-01		-4.5704E-02	1.8976E-02	.0000E 00	-1.4861E-02	1.9819E-02	-4.6847E-02	6.6365E-02
3 1	7.227	.163	1.1141E 01	2.9335E 01	2.6005E 01	-1.6173E 00	2.9477E 01	1.0998E 01	9.8395E 00
-84.96	1.0389E-01		-3.4684E-02	7.7681E-03	.0000E 00	-7.5473E-03	8.1009E-03	-3.5017E-02	4.3118E-02
4 1	7.584	.180	1.8901E 01	2.8729E 01	2.5121E 01	-6.4990E-01	2.8768E 01	1.2868E 01	8.4468E 00
-87.11	9.9687E-02		-8.8514E-02	1.4175E-03	.0000E 00	-3.0389E-03	1.4941E-03	-2.8891E-02	3.0085E-02
5 1	7.915	.196	1.3659E 01	2.4268E 01	2.4747E 01	-2.0331E-01	2.4272E 01	1.3655E 01	5.3584E 00
-88.91	9.7908E-02		-2.6105E-02	-1.1171E-03	.0000E 00	-9.4877E-04	-1.1081E-03	-2.6114E-02	2.5006E-02
6 1	8.319	.206	1.2687E 01	2.4651E 01	2.4990E 01	5.1268E-02	2.4651E 01	1.2657E 01	5.9972E 00
89.73	9.9064E-02		-2.6444E-02	-7.9168E-04	.0000E 00	2.3925E-04	-7.9107E-04	-2.6445E-02	2.5663E-02
1 2	6.668	.409	8.8884E 00	4.4736E 01	3.2603E 01	-1.2208E 01	4.8498E 01	5.1258E 00	2.1686E 01
-72.87	1.3524E-01		-5.5335E-02	2.8309E-02	.0000E 00	-5.6971E-02	3.7088E-02	-4.4115E-02	1.0120E-01
2 2	6.864	.440	1.1497E 01	3.8970E 01	2.7926E 01	-7.8670E 00	3.8544E 01	8.9837E 00	1.3310E 01
-71.88	1.1301E-01		-3.8332E-02	1.1771E-02	.0000E 00	-3.6713E-02	1.7776E-02	-4.4338E-02	6.2114E-02
3 2	7.136	.487	1.2335E 01	2.7962E 01	2.5904E 01	-2.9909E 00	2.8922E 01	1.1374E 01	8.7737E 00
-76.47	1.0341E-01		-3.1663E-02	4.8004E-03	.0000E 00	-1.8624E-02	7.0409E-03	-3.3903E-02	4.0944E-02
4 2	7.469	.543	1.2546E 01	2.6016E 01	2.4591E 01	-1.7264E 00	2.6253E 01	1.2309E 01	6.4720E 00
-82.22	9.7168E-02		-2.8108E-02	9.9047E-04	.0000E 00	-8.1033E-03	1.5441E-03	-2.8658E-02	3.0803E-02
5 2	7.853	.596	1.2731E 01	2.3731E 01	2.4070E 01	-6.1977E-01	2.3765E 01	1.2696E 01	5.5346E 00
-86.79	9.4692E-02		-2.6458E-02	-7.9241E-04	.0000E 00	-2.8922E-03	-7.1119E-04	-2.6539E-02	2.5828E-02
6 2	8.283	.634	1.2741E 01	2.4104E 01	2.4273E 01	9.7483E-02	2.4104E 01	1.2740E 01	5.6880E 00
89.61	9.5655E-02		-2.6907E-02	-3.9479E-04	.0000E 00	4.5492E-04	-3.9284E-04	-2.6909E-02	2.6516E-02
1 3	6.540	.651	2.6001E 01	3.2833E 01	3.4624E 01	-1.9192E 01	4.8911E 01	9.9231E 00	1.9494E 01
-50.05	1.4485E-01		-2.0120E-02	-4.1797E-03	.0000E 00	-8.9564E-02	3.3336E-02	-5.7635E-02	9.0971E-02

APPENDIX C-2

17KS12000

Booster Cavity

Axisymmetric Structural Analysis

Computer Printouts

I J/ ANGLE	COORDINATES X	Y	X	Y	STRESSES / STRAINS AXIAL Z	SHEAR X-Y	MAXIMUM	MINIMUM	MAX SHEAR
1 1	6.711	.235	3.4943E-01	1.9683E 01	1.6013E 01	-6.7356E-01	1.9706E 01	3.2599E-01	9.6902E 00
-88.01	5.6401E-02		-3.6547E-02	8.5641E-03	.0000E 00	-3.1433E-03	8.6188E-03	-3.6602E-02	4.5221E-02
2 1	6.957	.243	1.0219E 00	1.9015E 01	1.6014E 01	-6.3214E-01	1.9037E 01	9.9967E-01	9.0188E 00
-87.99	5.6406E-02		-3.4981E-02	7.0032E-03	.0000E 00	-2.9500E-03	7.0549E-03	-3.5033E-02	4.2088E-02
3 1	7.250	.253	1.7366E 00	1.8304E 01	1.6015E 01	-5.8195E-01	1.8324E 01	1.7162E 00	8.3040E 00
-87.99	5.6414E-02		-3.3317E-02	5.3393E-03	.0000E 00	-2.7158E-03	5.3869E-03	-3.3365E-02	3.8752E-02
4 1	7.573	.264	2.4273E 00	1.7613E 01	1.6015E 01	-5.3029E-01	1.7631E 01	2.4088E 00	7.6112E 00
-88.00	5.6412E-02		-3.1705E-02	3.7279E-03	.0000E 00	-2.4747E-03	3.7711E-03	-3.1748E-02	3.5519E-02
5 1	7.925	.277	3.0861E 00	1.6954E 01	1.6015E 01	-4.8500E-01	1.6971E 01	3.0691E 00	6.9509E 00
-88.00	5.6412E-02		-3.0168E-02	2.1911E-03	.0000E 00	-2.2633E-03	2.2306E-03	-3.0207E-02	3.2438E-02
6 1	8.319	.291	3.7260E 00	1.6315E 01	1.6016E 01	-4.4098E-01	1.6331E 01	3.7106E 00	6.3100E 00
-88.00	5.6415E-02		-2.8675E-02	6.9919E-04	.0000E 00	-2.0579E-03	7.3519E-04	-2.8711E-02	2.9447E-02
1 2	6.683	.703	5.5445E-01	1.9482E 01	1.6014E 01	-2.0129E 00	1.9693E 01	3.4274E-01	9.6753E 00
-84.00	5.6407E-02		-3.6072E-02	8.0913E-03	.0000E 00	-9.3937E-03	8.5853E-03	-3.6566E-02	4.5151E-02
2 2	6.930	.729	1.2159E 00	1.8821E 01	1.6014E 01	-1.8754E 00	1.9019E 01	1.0183E 00	9.0002E 00
-83.99	5.6408E-02		-3.4529E-02	6.5498E-03	.0000E 00	-8.7517E-03	7.0108E-03	-3.4990E-02	4.2001E-02
3 2	7.214	.758	1.8952E 00	1.8142E 01	1.6014E 01	-1.7298E 00	1.8324E 01	1.7131E 00	8.3055E 00
-83.99	5.6407E-02		-3.2944E-02	4.9653E-03	.0000E 00	-8.0724E-03	5.3903E-03	-3.3369E-02	3.8759E-02
4 2	7.533	.792	2.5686E 00	1.7471E 01	1.6015E 01	-1.5853E 00	1.7637E 01	2.4018E 00	7.6178E 00
-83.99	5.6411E-02		-3.1374E-02	3.3972E-03	.0000E 00	-7.3981E-03	3.7864E-03	-3.1763E-02	3.5550E-02
5 2	7.887	.829	3.2217E 00	1.6819E 01	1.6015E 01	-1.4466E 00	1.6972E 01	3.0695E 00	6.9510E 00
-83.99	5.6414E-02		-2.9852E-02	1.8756E-03	.0000E 00	-6.7509E-03	2.2307E-03	-3.0207E-02	3.2438E-02
6 2	8.279	.870	3.8499E 00	1.6192E 01	1.6016E 01	-1.3133E 00	1.6330E 01	3.7117E 00	6.3090E 00
-83.99	5.6415E-02		-2.8387E-02	4.1044E-04	.0000E 00	-6.1285E-03	7.3289E-04	-2.8709E-02	2.9442E-02
1 3	6.619	1.167	9.3129E-01	1.9104E 01	1.6014E 01	-3.3115E 00	1.9689E 01	3.4666E-01	9.6711E 00
-79.99	5.6406E-02		-3.5193E-02	7.2109E-03	.0000E 00	-1.5454E-02	8.5751E-03	-3.6557E-02	4.5132E-02

APPENDIX D

17KS12000

Axisymmetric Structural Analysis

Thermal Loading

Computer Printouts

I J/ ANGLE	COORDINATES R	Z	STRESSES / STRAINS RADIAL R	HOOP THETA	AXIAL Z	SHEAR R-Z	MAXIMUM	MINIMUM	MAX SHEAR
1 1	2.718	.559	-3.8093E 00	-2.0514E 01	6.9978E-02	-5.5381E-01	1.4749E-01	-3.8868E 00	2.0171E 00
-82.03			4.7405E-04	-3.8503E-02	9.5256E-03	-2.5845E-03	9.7065E-03	2.9318E-04	9.4133E-03
2 1	3.797	.756	-7.1058E 00	-1.4833E 01	6.2376E-01	-1.8004E 00	9.0477E-01	-7.3868E 00	4.1458E 00
-79.39			-9.7256E-03	-2.7756E-02	8.3099E-03	-7.0017E-03	8.9656E-03	-1.0381E-02	1.9347E-02
3 1	5.050	1.123	-7.7985E 00	-1.1484E 01	2.1062E-01	-2.6695E 00	1.0189E 00	-8.6067E 00	4.8128E 00
-73.16			-1.3149E-02	-2.1750E-02	5.5386E-03	-1.2458E-02	7.4245E-03	-1.5035E-02	2.2460E-02
4 1	6.319	1.668	-6.1856E 00	-8.2410E 00	-4.8114E-01	-4.1191E 00	1.7004E 00	-8.3371E 00	5.0188E 00
-62.42			-1.2673E-02	-1.7469E-02	7.0692E-04	-1.9222E-02	5.7272E-03	-1.7694E-02	2.3421E-02
5 1	7.319	2.313	-3.8151E 00	-5.6903E 00	-2.3389E 00	-5.1914E 00	2.1700E 00	-8.3180E 00	5.2440E 00
-49.06			-9.4905E-03	-1.3866E-02	-6.0319E-03	-2.4226E-02	4.4748E-03	-1.9997E-02	2.4472E-02
6 1	7.882	2.971	-9.9112E-01	-3.8303E 00	-5.2241E 00	-5.9185E 00	3.1779E 00	-9.3932E 00	6.2856E 00
-38.16			-3.8024E-03	-1.0427E-02	-1.3679E-02	-2.7620E-02	5.9254E-03	-2.3407E-02	2.9333E-02
7 1	8.208	3.575	2.6743E 00	-4.5558E 00	-1.6042E 01	-7.6395E 00	5.3966E 00	-1.8764E 01	1.2080E 01
-19.61			1.0480E-02	-6.3901E-03	-3.3190E-02	-3.8651E-02	1.6832E-02	-3.9543E-02	5.6375E-02
8 1	8.441	3.974	2.7808E 01	2.6095E 01	5.8433E 00	-2.1718E 01	4.1078E 01	-7.7263E 00	2.4402E 01
-31.43			1.8986E-03	-2.3981E-03	-5.0382E-02	-1.0134E-01	3.2561E-02	-8.1315E-02	1.1388E-01
1 2	2.433	1.497	-6.3908E-01	-1.2939E 01	1.3102E 00	5.6667E-01	1.4630E 00	-7.9184E-01	1.1274E 00
74.91			-1.8503E-03	-3.0260E-02	2.9982E-03	8.6445E-03	3.3546E-03	-1.9067E-03	5.2613E-03
2 2	3.116	1.874	-2.6738E 00	-7.8244E 00	1.6591E 00	-6.7793E-01	1.7627E 00	-2.7768E 00	2.2698E 00
-81.31			-9.0389E-03	-2.1058E-02	1.0698E-03	-3.1637E-03	1.3116E-03	-9.2807E-03	1.0592E-02
3 2	4.166	2.288	-2.2106E 00	-3.5283E 00	2.6398E 00	-1.4282E 00	3.0291E 00	-2.5999E 00	2.8145E 00
-74.75			-1.2413E-02	-1.5488E-02	-1.0956E-03	-6.6651E-03	-1.8727E-04	-1.3322E-02	1.3134E-02
4 2	5.257	2.800	-4.8130E-01	-2.2587E-01	2.8613E 00	-2.4496E 00	4.1854E 00	-1.7755E 00	2.9684E 00
-62.15			-1.2442E-02	-1.1846E-02	-4.6422E-03	-1.1432E-02	-1.6225E-03	-1.8461E-02	1.3839E-02
5 2	6.245	3.346	3.2265E 00	3.9459E 00	3.7298E 00	-3.4567E 00	6.9440E 00	1.2307E-02	3.4658E 00
-47.08			-1.0844E-02	-8.8657E-03	-9.3701E-03	-1.6131E-02	-1.8703E-03	-1.8044E-02	1.6174E-02

I J/ ANGLE	COORDINATES R	Z	STRESSES / STRAINS RADIAL R	HOOP THETA	AXIAL Z	SHEAR R-Z	MAXIMUM	MINIMUM	MAX SHEAR
5 17	3.036	26.137	1.9309E 01	4.9942E 01	4.4275E 01	-2.8164E-02	4.4275E 01	1.9309E 01	1.2483E 01
-89.94			-6.8459E-02	4.9730E-02	-1.0206E-02	-1.3144E-04	-1.0206E-02	-6.8459E-02	5.8252E-02
6 17	4.608	26.151	3.4183E 01	5.6153E 01	4.5123E 01	-1.0208E-01	4.5124E 01	3.4182E 01	5.4710E 00
-89.47			-2.4222E-02	1.7043E-02	-8.6954E-03	-4.7638E-04	-8.6932E-03	-3.4225E-02	2.5531E-02
7 17	6.180	26.151	3.8768E 01	5.1643E 01	4.6512E 01	-1.3076E-01	4.6514E 01	3.8766E 01	3.8741E 00
-89.03			-2.4494E-02	5.5475E-03	-6.4251E-03	-6.1022E-04	-6.4200E-03	-2.4499E-02	1.8079E-02
8 17	7.761	26.137	4.0686E 01	4.9806E 01	4.8355E 01	-1.7259E-01	4.8358E 01	4.0652E 01	3.8532E 00
-88.72			-2.1803E-02	-1.5287E-04	-3.5393E-03	-8.0543E-04	-3.5302E-03	-2.1812E-02	1.7982E-02
5 18	3.036	27.810	1.9506E 01	6.9921E 01	4.4191E 01	1.1161E-01	4.4192E 01	1.9506E 01	1.2343E 01
89.74			-6.8051E-02	4.9583E-02	-1.0452E-02	5.2087E-04	-1.0451E-02	-6.8052E-02	5.7601E-02
6 18	4.608	27.801	3.4086E 01	5.6012E 01	4.4961E 01	3.0961E-01	4.4970E 01	3.4078E 01	5.4461E 00
88.37			-2.4141E-02	1.7019E-02	-8.7668E-03	1.4449E-03	-8.7463E-03	-3.4161E-02	2.5415E-02
7 18	6.180	27.801	3.8729E 01	5.1591E 01	4.6485E 01	4.3795E-01	4.6489E 01	3.8704E 01	3.8879E 00
86.77			-2.4470E-02	5.5401E-03	-6.4421E-03	2.0438E-03	-6.3844E-03	-2.4528E-02	1.8144E-02
8 18	7.781	27.810	4.0581E 01	4.9734E 01	4.8299E 01	5.4992E-01	4.8338E 01	4.0542E 01	3.8980E 00
85.94			-2.1510E-02	-1.5349E-04	-3.8014E-03	2.5663E-03	-3.4105E-03	-2.1601E-02	1.8191E-02
5 19	3.037	29.456	1.9009E 01	6.9308E 01	4.3692E 01	2.8333E-01	4.3696E 01	1.9006E 01	1.2345E 01
89.34			-6.7955E-02	4.9408E-02	-1.0361E-02	1.3222E-03	-1.0354E-02	-6.7963E-02	5.7609E-02
6 19	4.609	29.442	3.3883E 01	5.5685E 01	4.4618E 01	7.0545E-01	4.4664E 01	3.3836E 01	5.4140E 00
86.26			-2.3941E-02	1.6932E-02	-8.8912E-03	3.2921E-03	-8.7835E-03	-3.4049E-02	2.5268E-02
7 19	6.181	29.442	3.8423E 01	5.1220E 01	4.6027E 01	1.0191E 00	4.6161E 01	3.8289E 01	3.9364E 00
82.80			-2.4337E-02	5.5224E-03	-6.5935E-03	4.7556E-03	-6.2804E-03	-2.4650E-02	1.8370E-02
8 19	7.762	29.456	4.0254E 01	4.9388E 01	4.7891E 01	1.2740E 00	4.8098E 01	4.0048E 01	4.0250E 00
80.77			-2.1465E-02	-1.6327E-04	-3.6476E-03	5.9452E-03	-3.1648E-03	-2.1948E-02	1.8784E-02
5 20	3.037	31.072	1.9049E 01	6.8490E 01	4.2878E 01	4.4117E-01	4.2886E 01	1.9041E 01	1.1923E 01
88.94			-6.6626E-02	4.8736E-02	-1.1025E-02	2.0588E-03	-1.1006E-02	-6.6645E-02	5.8639E-02

I J/ ANGLE	COORDINATES R	Z	STRESSES / STRAINS RADIAL R	HOOP THETA	AXIAL Z	SHEAR R-Z	MAXIMUM	MINIMUM	MAX SHEAR
7 23	6.210	35.926	3.4836E 01	4.6767E 01	4.1009E 01	3.6795E 00	4.2725E 01	3.3120E 01	4.8029E 00
66.00			-2.2666E-02	5.1746E-03	-8.2608E-03	1.7171E-02	+4.2568E-03	-2.6670E-02	2.2413E-02
8 23	7.763	35.938	3.6208E 01	4.8226E 01	4.3628E 01	4.6472E 00	4.8783E 01	3.3950E 01	5.9164E 00
64.12			-2.1219E-02	-1.6992E-04	-4.1318E-03	2.1687E-02	1.1294E-03	-2.6481E-02	2.7610E-02
5 24	3.069	37.624	1.7149E 01	5.9881E 01	3.8325E 01	1.2201E 00	3.5406E 01	1.7067E 01	9.1697E 00
86.18			-5.7054E-02	4.2656E-02	-1.4643E-02	5.6939E-03	-1.4453E-02	-5.7244E-02	4.2792E-02
6 24	4.679	37.867	2.3680E 01	4.8307E 01	3.6611E 01	3.0759E 00	3.7779E 01	2.8512E 01	4.6338E 00
69.20			-2.8672E-02	1.4790E-02	-1.2499E-02	1.4384E-02	-9.7738E-03	-3.1398E-02	2.1624E-02
7 24	6.242	37.829	3.3013E 01	4.4593E 01	3.8651E 01	4.8479E 00	4.1182E 01	3.0482E 01	5.3505E 00
60.89			-2.2041E-02	4.9788E-03	-8.8878E-03	2.1284E-02	-2.9799E-03	-2.7949E-02	2.4969E-02
8 24	7.778	37.860	3.4397E 01	4.3381E 01	4.1597E 01	5.6988E 00	4.4738E 01	3.1856E 01	6.7408E 00
61.14			-2.1154E-02	-1.9191E-04	-4.3834E-03	2.6598E-02	2.9746E-03	-2.8482E-02	3.1487E-02
5 25	3.114	39.411	1.7341E 01	5.6377E 01	3.1905E 01	1.4668E 00	3.2051E 01	1.7195E 01	7.4282E 00
84.31			-5.1369E-02	3.9715E-02	-1.7386E-02	6.8438E-03	-1.7045E-02	-5.1710E-02	3.4668E-02
6 25	4.765	39.187	2.7748E 01	4.8105E 01	3.3295E 01	4.1528E 00	3.8518E 01	2.8825E 01	4.9948E 00
61.88			-2.6696E-02	1.3811E-02	-1.3745E-02	1.9380E-02	-8.8668E-03	-3.1875E-02	2.3309E-02
7 25	6.304	39.062	3.1113E 01	4.2421E 01	3.6459E 01	5.5424E 00	3.9939E 01	2.7633E 01	6.1532E 00
57.87			-2.1677E-02	4.7069E-03	-9.2043E-03	2.5865E-02	-1.0831E-03	-2.9798E-02	2.8715E-02
8 25	7.797	39.036	3.1978E 01	4.0938E 01	3.9025E 01	6.7575E 00	4.3122E 01	2.7881E 01	7.6209E 00
58.77			-2.1147E-02	-2.3911E-04	-4.7045E-03	3.1535E-02	4.8665E-03	-3.0708E-02	3.5564E-02
4 26	2.462	41.717	8.5951E 00	6.2110E 01	2.2308E 01	3.2430E 00	2.3036E 01	7.8668E 00	7.5847E 00
77.34			-5.9202E-02	6.5667E-02	-2.7205E-02	1.5134E-02	-2.5505E-02	-6.0901E-02	3.5395E-02
5 26	3.481	41.045	1.6868E 01	4.8410E 01	2.6789E 01	3.6548E 00	2.7989E 01	1.6667E 01	6.1611E 00
71.81			-4.1781E-02	3.1816E-02	-1.8632E-02	1.7053E-02	-1.5831E-02	-4.4583E-02	2.8762E-02
6 26	4.962	40.709	2.5984E 01	4.2294E 01	3.1143E 01	5.7753E 00	3.4889E 01	2.2238E 01	6.3252E 00
57.03			-2.5584E-02	1.2473E-02	-1.3546E-02	2.6961E-02	-4.8060E-03	-3.4323E-02	2.9517E-02

I J/ ANGLE	COORDINATES R	Z	STRESSES / STRAINS RADIAL R	HOOP THETA	AXIAL Z	SHEAR R-Z	MAXIMUM	MINIMUM	MAX SHEAR
8 32	8.125	47.455	1.4852E 01	2.5451E 01	2.5498E 01	9.1973E 00	3.0802E 01	9.5481E 00	1.0627E 01
60.03			-2.5580E-02	-8.4733E-04	-7.3784E-04	4.2921E-02	1.1637E-02	-3.7958E-02	4.9592E-02
6 33	6.767	48.789	1.1284E 01	3.1968E 01	3.3874E 01	1.8799E 01	3.9400E 01	5.4880E 00	1.6971E 01
68.52			-4.2881E-02	5.3743E-03	9.1271E-03	5.9728E-02	2.2722E-02	-5.6476E-02	7.9198E-02
7 33	7.440	48.829	1.2508E 01	2.6419E 01	2.6531E 01	8.5607E 00	3.0586E 01	8.4544E 00	1.1066E 01
64.66			-3.0837E-02	1.6209E-03	1.8830E-03	3.9950E-02	1.1343E-02	-4.0297E-02	5.1639E-02
8 33	8.167	48.334	1.4479E 01	2.4858E 01	2.4808E 01	8.6613E 00	2.9728E 01	9.5593E 00	1.0084E 01
60.40			-2.5195E-02	-9.7741E-04	-1.0941E-03	4.0420E-02	1.0388E-02	-3.6674E-02	4.7059E-02
6 34	6.902	49.384	7.4273E 00	3.0887E 01	3.5387E 01	7.7413E 00	3.7387E 01	5.4270E 00	1.5980E 01
78.51			-4.9726E-02	5.0126E-03	1.5514E-02	3.6126E-02	2.0181E-02	-5.4393E-02	7.4574E-02
7 34	7.523	49.276	1.1112E 01	2.8223E 01	2.8751E 01	8.2151E 00	2.9434E 01	7.4889E 00	1.1003E 01
68.85			-3.1565E-02	1.3603E-03	2.5909E-03	3.8337E-02	1.1186E-02	-4.0160E-02	5.1346E-02
8 34	8.194	49.186	1.3023E 01	2.3435E 01	2.3485E 01	8.2966E 00	2.8016E 01	8.4320E 00	9.7919E 00
61.04			-2.5341E-02	-1.0463E-03	-1.0706E-03	3.8717E-02	9.6420E-03	-3.6054E-02	4.5696E-02
6 35	6.921	50.036	1.8665E 00	2.4393E 01	2.8127E 01	3.2882E 00	2.8532E 01	1.4618E 00	1.3536E 01
82.98			-4.7105E-02	5.4869E-03	1.4169E-02	1.5331E-02	1.5114E-02	-4.8049E-02	6.3143E-02
7 35	7.554	50.005	7.4271E 00	2.3311E 01	2.6389E 01	6.6063E 00	2.7557E 01	5.2590E 00	1.1149E 01
71.83			-2.5539E-02	1.5241E-03	6.3720E-03	3.0829E-02	1.1431E-02	-4.0598E-02	5.2029E-02
8 35	8.207	49.994	9.4816E 00	2.0692E 01	2.1168E 01	7.8913E 00	2.4944E 01	5.9059E 00	9.5191E 00
63.56			-2.6724E-02	-1.0322E-03	7.8053E-05	3.6426E-02	8.8882E-03	-3.5534E-02	4.4422E-02
6 36	6.927	50.734	1.2958E 00	2.1917E 01	2.3601E 01	1.5340E 00	2.3706E 01	1.2900E 00	1.1208E 01
86.07			-4.2472E-02	5.4124E-03	9.3405E-03	7.1586E-03	9.5866E-03	-4.2718E-02	5.2305E-02
7 36	7.566	50.714	4.0403E 00	2.0135E 01	2.2238E 01	4.3707E 00	2.3233E 01	3.0449E 00	1.0094E 01
77.17			-3.5925E-02	1.6304E-03	6.5356E-03	2.0397E-02	8.8581E-03	-3.8248E-02	4.7106E-02
8 36	8.212	50.730	6.8534E 00	1.8363E 01	1.9281E 01	6.2162E 00	2.1831E 01	4.2735E 00	8.7789E 00
67.46			-2.7858E-02	-1.0032E-03	1.0704E-03	2.9009E-02	7.0901E-03	-3.3878E-02	4.0968E-02

APPENDIX E

17KS12000

Axisymmetric Structural Analysis

Acceleration Loading

Computer Printouts

I	J	R-COORDINATE	Z-COORDINATE	R-DISPLACEMENT	Z-DISPLACEMENT
1	1	2.2500	.0000	-4.8931E-02	1.1978E-01
2	1	3.3900	.0470	-4.2566E-02	1.0965E-01
3	1	4.7800	.2810	-4.0454E-02	9.4160E-02
4	1	6.1900	.7360	-3.7474E-02	7.3446E-02
5	1	7.5910	1.4380	-2.9534E-02	4.7474E-02
6	1	8.2560	2.1600	-1.9386E-02	2.3425E-02
7	1	8.4370	2.9360	-1.0479E-02	2.6508E-02
8	1	8.5370	3.6000	-3.6408E-03	1.6039E-02
9	1	8.5370	3.9000	1.5100E-04	5.7265E-03
1	2	2.2500	1.0000	-4.1340E-02	1.2827E-01
2	2	2.9817	1.1889	-3.4384E-02	1.2383E-01
3	2	4.0369	1.5080	-2.9559E-02	1.1398E-01
4	2	5.1919	1.9681	-2.5299E-02	9.8609E-02
5	2	6.3014	2.5349	-2.0482E-02	7.8108E-02
6	2	7.1295	3.1199	-1.5547E-02	5.8511E-02
7	2	7.7041	3.6697	-1.0764E-02	4.1899E-02
8	2	8.1649	4.0945	-4.2788E-03	2.5258E-02
9	2	8.5370	4.3000	1.5345E-04	8.7028E-03
1	3	2.2500	1.6000	-3.7255E-02	1.3213E-01
2	3	2.2500	2.2000	-3.2052E-02	1.3524E-01
3	3	3.1941	2.5976	-2.3858E-02	1.2911E-01
4	3	4.2398	3.0829	-1.8798E-02	1.1767E-01
5	3	5.2932	3.6154	-1.4570E-02	1.0097E-01
6	3	6.2562	4.1142	-1.0530E-02	8.0687E-02
7	3	7.0952	4.5298	-5.7793E-03	5.8367E-02
8	3	7.8416	4.8089	-1.2653E-03	3.2614E-02
9	3	8.5370	4.9000	1.6642E-04	5.6661E-03
2	4	2.2500	2.9000	-2.8947E-02	1.3722E-01
3	4	2.2500	3.6000	-2.3812E-02	1.3921E-01
4	4	3.2788	4.1830	-1.5634E-02	1.3170E-01
5	4	4.3756	4.7291	-1.0549E-02	1.1786E-01
6	4	5.5072	5.1924	-6.5876E-03	9.6903E-02
7	4	6.5789	5.5271	-3.1689E-03	7.0249E-02
8	4	7.5794	5.7111	-8.3899E-04	3.9580E-02
9	4	8.5370	5.7000	1.3562E-04	5.6156E-03
3	5	2.2500	4.4000	-2.1327E-02	1.3916E-01
4	5	2.2500	5.2000	-1.6832E-02	1.3992E-01
5	5	3.4234	5.9571	-8.9759E-03	1.3008E-01
6	5	4.8180	6.3990	-4.5693E-03	1.0930E-01

SLUMP

I J/ ANGLE	COORDINATES R	Z	STRESSES / STRAINS RADIAL R	HOOP THETA	AXIAL Z	SHEAR R-Z	MAXIMUM	MINIMUM	MAX SHEAR
1 1	2.718	.559	-1.1098E 00	-6.1224E 00	-4.8687E-01	-5.9546E-02	-4.8123E-01	-1.1154E 00	3.1708E-01
-84.59			6.1019E-03	-1.5071E-02	8.7328E-03	-6.0302E-04	8.7567E-03	6.0781E-03	2.6786E-03
2 1	3.797	.756	-2.0992E 00	-4.5953E 00	-3.6989E-01	-4.4072E-01	-2.6406E-01	-2.2051E 00	9.7051E-01
-76.50			9.9889E-04	-9.5439E-03	8.3033E-03	-3.7230E-03	8.7503E-03	5.5185E-04	8.1985E-03
3 1	5.050	1.123	-2.2580E 00	-3.7117E 00	-6.0193E-01	-8.6188E-01	-2.3477E-01	-2.6251E 00	1.1952E 00
-66.93			-3.8290E-04	-6.5233E-03	6.6119E-03	-7.2808E-03	8.1627E-03	-1.9337E-03	1.0096E-02
4 1	6.319	1.668	-1.7961E 00	-2.9214E 00	-9.6060E-01	-1.2928E 00	-1.9969E-02	-2.7367E 00	1.3584E 00
-53.96			3.1283E-04	-4.4402E-03	3.8416E-03	-1.0919E-02	7.8147E-03	-3.6602E-03	1.1475E-02
5 1	7.319	2.313	-1.1980E 00	-2.4135E 00	-1.6553E 00	-1.6289E 00	2.1820E-01	-3.0715E 00	1.6449E 00
-41.01			2.2698E-03	-2.8639E-03	3.3857E-04	-1.3760E-02	8.2517E-03	-5.6433E-03	1.3895E-02
6 1	7.882	2.971	-1.2230E 00	-2.5791E 00	-3.0478E 00	-2.1682E 00	2.1699E-01	-4.4878E 00	2.3524E 00
-33.59			4.0169E-03	-1.7112E-03	-3.6910E-03	-1.8316E-02	1.0099E-02	-9.7731E-03	1.9872E-02
7 1	8.208	3.575	-1.5705E 00	-3.7996E 00	-5.5725E 00	-2.8128E 00	-1.1956E-01	-7.0235E 00	3.4520E 00
-27.29			8.5568E-03	-8.5830E-04	-8.3468E-03	-2.3762E-02	1.4685E-02	-1.4475E-02	2.9161E-02
8 1	8.441	3.974	-1.7105E 00	-4.1306E 00	-7.1611E 00	-5.0407E 00	1.2944E 00	-1.0166E 01	5.7302E 00
-30.80			1.0111E-02	-1.1064E-04	-1.2911E-02	-4.2581E-02	2.2804E-02	-2.5603E-02	4.8407E-02
1 2	2.433	1.497	-7.9438E-01	-6.1084E 00	-1.1668E 00	9.5611E-03	-7.9414E-01	-1.1670E 00	1.8645E-01
1.47			7.5594E-03	-1.4886E-02	6.9864E-03	8.0768E-05	7.5604E-03	5.9864E-03	1.5751E-03
2 2	3.116	1.874	-1.8670E 00	-4.4813E 00	-1.0052E 00	-3.3585E-01	-7.7564E-01	-1.4965E 00	3.6045E-01
-55.64			4.1690E-03	-9.4078E-03	5.2745E-03	-2.8371E-03	6.2442E-03	3.1993E-03	3.0449E-03
3 2	4.166	2.288	-1.7388E 00	-3.4399E 00	-1.0932E 00	-8.5621E-01	-5.0096E-01	-2.3310E 00	9.1504E-01
-55.33			1.4108E-03	-5.7744E-03	4.1378E-03	-7.2329E-03	6.6392E-03	-1.0907E-03	7.7299E-03
4 2	5.257	2.800	-1.7076E 00	-2.8035E 00	-1.3242E 00	-1.4261E 00	-7.6930E-02	-2.9549E 00	1.4390E 00
-48.83			8.9981E-04	-3.7291E-03	2.5195E-03	-1.2047E-02	7.7876E-03	-4.3682E-03	1.2156E-02
5 2	6.245	3.346	-1.6138E 00	-2.4670E 00	-1.6788E 00	-1.9666E 00	3.2064E-01	-3.6132E 00	1.9669E 00
-44.53			1.1715E-03	-2.4326E-03	8.9679E-04	-1.6613E-02	9.3419E-03	-7.2737E-03	1.6616E-02

APPENDIX F

17KS12000

Axisymmetric structural Analysis

Pressurization Loading

Computer Printouts

I J/ ANGLE	COORDINATES R	Z	RADIAL R	HOOP THETA	STRESSES / STRAINS AXIAL Z	SHEAR R-Z	MAXIMUM	MINIMUM	MAX SHEAR
1 1	2.718	.559	-1.0270E 03	-1.1466E 03	-9.9930E 02	-4.0797E 00	-9.9871E 02	-1.0276E 03	1.4443E 01
-81.60			3.6759E-03	-2.0448E-02	9.6124E-03	-1.6597E-03	9.6320E-03	3.7562E-03	5.8758E-03
2 1	3.797	.756	-1.0508E 03	-1.1066E 03	-9.9879E 02	-1.0759E 01	-9.9376E 02	-1.0528E 03	2.9511E 01
-79.31			-2.4316E-03	-1.3786E-02	8.7477E-03	-4.3771E-03	9.1609E-03	-2.8447E-03	1.2006E-02
3 1	5.050	1.123	-1.0561E 03	-1.0829E 03	-9.9822E 02	-1.9140E 01	-9.9246E 02	-1.0618E 03	3.4681E 01
-73.25			-4.0326E-03	-1.0098E-02	7.1333E-03	-7.7866E-03	8.3049E-03	-5.8042E-03	1.4109E-02
4 1	6.319	1.668	-1.0468E 03	-1.0621E 03	-1.0036E 03	-2.9607E 01	-9.8853E 02	-1.0619E 03	3.6667E 01
-63.08			-4.4443E-03	-7.5513E-03	4.3658E-03	-1.2045E-02	7.4142E-03	-7.5027E-03	1.4917E-02
5 1	7.319	2.313	-1.0317E 03	-1.0454E 03	-1.0158E 03	-3.8909E 01	-9.8402E 02	-1.0634E 03	3.9710E 01
-50.76			-2.6936E-03	-5.4934E-03	5.3846E-04	-1.5829E-02	6.9985E-03	-9.1566E-03	1.6155E-02
6 1	7.882	2.972	-1.0237E 03	-1.0413E 03	-1.0399E 03	-4.8221E 01	-9.8288E 02	-1.0807E 03	4.8900E 01
-40.22			-7.5180E-05	-3.6560E-03	-3.3780E-03	-1.9617E-02	8.2202E-03	-1.1673E-02	1.9894E-02
7 1	8.208	3.575	-1.0186E 03	-1.0591E 03	-1.0934E 03	-5.9036E 01	-9.8612E 02	-1.1259E 03	6.9866E 01
-28.84			6.4623E-03	-1.7786E-03	-8.7375E-03	-2.4017E-02	1.3074E-02	-1.5349E-02	2.8423E-02
8 1	8.441	3.974	-9.9070E 02	-1.0402E 03	-1.1325E 03	-1.3233E 02	-9.1146E 02	-1.2117E 03	1.5012E 02
-30.91			1.0241E-02	1.7010E-04	-1.8595E-02	-5.3834E-02	2.6358E-02	-3.4712E-02	6.1070E-02
1 2	2.433	1.497	-1.0054E 03	-1.0955E 03	-9.9030E 02	3.7393E 00	-9.8942E 02	-1.0063E 03	8.4383E 00
76.85			2.0375E-03	-1.5691E-02	5.7149E-03	1.5212E-03	5.8927E-03	2.4598E-03	3.4329E-03
2 2	3.116	1.874	-1.0201E 03	-1.0593E 03	-9.8775E 02	-4.9229E 00	-9.8702E 02	-1.0209E 03	1.6926E 01
-81.55			-1.9983E-03	-9.9601E-03	4.5898E-03	-2.0027E-03	4.7386E-03	-2.1472E-03	6.8858E-03
3 2	4.166	2.288	-1.0199E 03	-1.0307E 03	-9.8207E 02	-9.5760E 00	-9.7979E 02	-1.0222E 03	2.1191E 01
-76.57			-4.2905E-03	-6.4830E-03	3.4000E-03	-3.8957E-03	3.8652E-03	-4.7557E-03	8.6209E-03
4 2	5.257	2.800	-1.0102E 03	-1.0075E 03	-9.7772E 02	-1.6002E 01	-9.7116E 02	-1.0168E 03	2.2811E 01
-67.73			-4.8395E-03	-4.2834E-03	1.7740E-03	-6.5100E-03	3.1073E-03	-6.1727E-03	9.2800E-03
5 2	6.245	3.346	-9.9470E 02	-9.8509E 02	-9.7343E 02	-2.1452E 01	-9.6013E 02	-1.0080E 03	2.3943E 01
-58.18			-4.5316E-03	-2.5759E-03	-2.0521E-04	-8.7270E-03	2.5019E-03	-7.2387E-03	9.7406E-03

I J/ ANGLE	COORDINATES R	Z	STRESSES / STRAINS RADIAL R	HOOP THETA	AXIAL Z	SHEAR R-Z	MAXIMUM	MINIMUM	MAX SHEAR
5 17	3.036	26.137	-8.7302E 02	-5.4004E 02	-7.1626E 02	-2.3159E-01	-7.1626E 02	-8.7302E 02	7.8378E 01
-89.92			-3.5653E-02	3.2078E-02	-3.7670E-03	-9.4214E-05	-3.7670E-03	-3.5653E-02	3.1886E-02
6 17	4.608	26.151	-7.7533E 02	-6.3115E 02	-7.1142E 02	-7.9236E-01	-7.1141E 02	-7.7534E 02	3.1963E 01
-89.29			-1.5972E-02	1.3355E-02	-2.9731E-03	-3.2235E-04	-2.9711E-03	-1.5974E-02	1.3003E-02
7 17	6.180	26.151	-7.4492E 02	-6.6077E 02	-7.0285E 02	-1.0036E 00	-7.0282E 02	-7.4494E 02	2.1060E 01
-88.63			-1.0325E-02	6.7903E-03	-1.7674E-03	-4.0828E-04	-1.7628E-03	-1.0330E-02	8.5676E-03
8 17	7.751	26.137	-7.3277E 02	-6.7343E 02	-6.9207E 02	-1.3638E 00	-6.9202E 02	-7.3281E 02	2.0394E 01
-88.08			-8.5185E-03	3.5520E-03	-2.4031E-04	-3.5469E-04	-2.3102E-04	-8.5278E-03	8.2968E-03
5 18	3.036	27.810	-8.7172E 02	-5.4013E 02	-7.1669E 02	6.3075E-01	-7.1668E 02	-8.7173E 02	7.7522E 01
89.77			-3.5439E-02	3.2010E-02	-3.9029E-03	2.5660E-04	-3.9024E-03	-3.5440E-02	3.1538E-02
6 18	4.608	27.801	-7.7564E 02	-6.3169E 02	-7.1214E 02	1.7670E 00	-7.1209E 02	-7.7569E 02	3.1800E 01
88.41			-1.5931E-02	1.3350E-02	-3.0143E-03	7.1887E-04	-3.0043E-03	-1.5941E-02	1.2937E-02
7 18	6.180	27.801	-7.4622E 02	-6.6119E 02	-7.0338E 02	2.4724E 00	-7.0323E 02	-7.4537E 02	2.1068E 01
86.63			-1.0303E-02	6.7939E-03	-1.7916E-03	1.0058E-03	-1.7620E-03	-1.0333E-02	8.5708E-03
8 18	7.751	27.810	-7.3251E 02	-6.7313E 02	-6.9172E 02	3.0919E 00	-6.9149E 02	-7.3275E 02	2.0629E 01
85.69			-8.5208E-03	3.5592E-03	-2.2345E-04	1.2578E-03	-1.7605E-04	-8.5682E-03	8.3921E-03
5 19	3.037	29.456	-8.7478E 02	-5.4357E 02	-7.1958E 02	1.6884E 00	-7.1956E 02	-8.7480E 02	7.7621E 01
89.38			-3.5423E-02	3.1949E-02	-3.8529E-03	6.8688E-04	-3.8492E-03	-3.5427E-02	3.1578E-02
6 19	4.609	29.442	-7.7689E 02	-6.3360E 02	-7.1425E 02	4.2000E 00	-7.1396E 02	-7.7717E 02	3.1604E 01
84.18			-1.5831E-02	1.3316E-02	-3.0876E-03	1.7086E-03	-3.0306E-03	-1.5888E-02	1.2857E-02
7 19	6.181	29.442	-7.4669E 02	-6.6295E 02	-7.0853E 02	6.0104E 00	-7.0467E 02	-7.4755E 02	2.1440E 01
81.86			-1.0242E-02	6.7915E-03	-1.8692E-03	2.4452E-03	-1.6944E-03	-1.0417E-02	8.7223E-03
8 19	7.752	29.456	-7.3484E 02	-6.7558E 02	-6.9465E 02	7.4904E 00	-6.9330E 02	-7.3619E 02	2.1444E 01
79.78			-8.4901E-03	3.5641E-03	-3.1548E-04	3.0472E-03	-4.0736E-05	-8.7648E-03	8.7241E-03
5 20	3.037	31.072	-8.7436E 02	-5.4824E 02	-7.2452E 02	2.6820E 00	-7.2447E 02	-8.7441E 02	7.4971E 01
84.97			-3.4716E-02	3.1621E-02	-4.2358E-03	1.0911E-03	-4.2260E-03	-3.4726E-02	3.0500E-02

I J/ ANGLE	COORDINATES R	Z	STRESSES / STRAINS RADIAL R	HOOP THETA	AXIAL Z	SHEAR R-Z	MAXIMUM	MINIMUM	MAX SHEAR
7 23	6.210	35.926	-7.6802E 02	-6.8905E 02	-7.3609E 02	2.2838E 01	-7.2419E 02	-7.7992E 02	2.7867E 01
62.48			-9.3535E-03	6.7114E-03	-2.8569E-03	9.2910E-03	-4.3668E-04	-1.1774E-02	1.1337E-02
8 23	7.763	35.938	-7.5875E 02	-6.9942E 02	-7.2012E 02	2.8629E 01	-7.0490E 02	-7.7397E 02	3.4536E 01
62.00			-8.4318E-03	3.6372E-03	-5.7325E-04	1.1647E-02	2.5225E-03	-1.1528E-02	1.4050E-02
5 24	3.069	37.624	-8.8521E 02	-5.9910E 02	-7.7146E 02	7.6784E 00	-7.7095E 02	-8.8573E 02	5.7390E 01
86.16			-2.9580E-02	2.8619E-02	-6.4424E-03	3.1237E-03	-6.3374E-03	-2.9685E-02	2.3348E-02
6 24	4.679	37.567	-8.0107E 02	-6.7673E 02	-7.6385E 02	1.9386E 01	-7.5533E 02	-8.0929E 02	2.6978E 01
67.03			-1.2925E-02	1.2367E-02	-5.2926E-03	7.8866E-03	-3.6213E-03	-1.4597E-02	1.0975E-02
7 24	6.242	37.529	-7.7900E 02	-7.0189E 02	-7.5059E 02	2.8693E 01	-7.3278E 02	-7.9681E 02	3.2015E 01
58.17			-9.0219E-03	6.6624E-03	-3.2449E-03	1.1673E-02	3.7878E-04	-1.2646E-02	1.3024E-02
8 24	7.775	37.560	-7.7022E 02	-7.1065E 02	-7.3201E 02	3.5575E 01	-7.1073E 02	-7.9150E 02	4.0380E 01
59.12			-8.4511E-03	3.6661E-03	-6.7938E-04	1.4473E-02	3.6488E-03	-1.2779E-02	1.6428E-02
5 25	3.114	39.411	-8.8284E 02	-6.1969E 02	-7.9274E 02	9.0304E 00	-7.9185E 02	-8.8374E 02	4.6945E 01
84.33			-2.6420E-02	2.7108E-02	-8.0925E-03	3.6738E-03	-7.9102E-03	-2.6602E-02	1.8692E-02
6 25	4.765	39.187	-8.1276E 02	-6.9645E 02	-7.8503E 02	2.6263E 01	-7.6919E 02	-8.2859E 02	2.9699E 01
58.92			-1.1762E-02	1.1897E-02	-6.1213E-03	1.0688E-02	-2.9006E-03	-1.4983E-02	1.2082E-02
7 25	6.304	39.062	-7.8975E 02	-7.1445E 02	-7.6447E 02	3.5465E 01	-7.3946E 02	-8.1476E 02	3.7651E 01
54.81			-8.7280E-03	6.5887E-03	-3.5849E-03	1.4428E-02	1.5020E-03	-1.3815E-02	1.5317E-02
8 25	7.797	39.036	-7.8427E 02	-7.2465E 02	-7.4778E 02	4.3294E 01	-7.1904E 02	-8.1300E 02	4.6982E 01
56.43			-8.4092E-03	3.7179E-03	-9.8700E-04	1.7613E-02	4.8584E-03	-1.4258E-02	1.9113E-02
4 26	2.462	41.717	-9.4166E 02	-5.7479E 02	-8.5285E 02	2.1270E 01	-8.4802E 02	-9.4649E 02	4.9235E 01
77.20			-3.1733E-02	4.2892E-02	-1.3668E-02	8.6532E-03	-1.2686E-02	-3.2715E-02	2.0030E-02
5 26	3.481	41.045	-8.8484E 02	-6.7081E 02	-8.2590E 02	2.3152E 01	-8.1789E 02	-8.9285E 02	3.7478E 01
70.92			-2.0888E-02	2.2649E-02	-8.8987E-03	9.4189E-03	-7.2701E-03	-2.2517E-02	1.5247E-02
6 26	4.962	40.709	-8.2314E 02	-7.1334E 02	-7.9840E 02	3.6832E 01	-7.7192E 02	-8.4962E 02	3.8853E 01
54.28			-1.1119E-02	1.1214E-02	-6.0876E-03	1.4984E-02	-6.9997E-04	-1.6506E-02	1.5806E-02

I J/ ANGLE	COORDINATES R	Z	STRESSES / STRAINS RADIAL R	HOOP THETA	AXIAL Z	SHEAR R-Z	MAXIMUM	MINIMUM	MAX SHEAR
8 32	8.125	47.455	-8.9728E 02	-8.2331E 02	-8.3845E 02	6.0730E 01	-7.9822E 02	-9.3451E 02	6.8145E 01
58.49			-1.1304E-02	3.7425E-03	1.2718E-03	2.4706E-02	8.8453E-03	-1.8877E-02	2.7723E-02
6 33	6.767	48.789	-9.2696E 02	-7.8355E 02	-7.8583E 02	8.2147E 01	-7.4810E 02	-9.6469E 02	1.0829E 02
65.33			-2.1620E-02	7.5509E-03	7.0877E-03	3.3419E-02	1.4762E-02	-2.9295E-02	4.4057E-02
7 33	7.440	48.529	-9.1810E 02	-8.2009E 02	-8.3107E 02	5.5420E 01	-8.0412E 02	-9.4505E 02	7.0461E 01
64.07			-1.4680E-02	5.2560E-03	3.0226E-03	2.2546E-02	8.5040E-03	-2.0161E-02	2.8665E-02
8 33	8.167	48.334	-9.0499E 02	-8.3141E 02	-8.4304E 02	5.7024E 01	-8.0918E 02	-9.3891E 02	6.4895E 01
59.26			-1.1314E-02	3.6535E-03	1.2888E-03	2.3198E-02	8.1879E-03	-1.8213E-02	2.6401E-02
6 34	6.902	49.384	-9.5205E 02	-7.9142E 02	-7.7560E 02	5.0390E 01	-7.6223E 02	-9.6542E 02	1.0160E 02
78.13			-2.5333E-02	7.3410E-03	1.0557E-02	2.0500E-02	1.3278E-02	-2.8054E-02	4.1332E-02
7 34	7.523	49.276	-9.2863E 02	-8.2909E 02	-8.3739E 02	5.4648E 01	-8.1182E 02	-9.5420E 02	7.1187E 01
64.93			-1.5124E-02	5.1229E-03	3.4350E-03	2.2232E-02	8.6356E-03	-2.0325E-02	2.8961E-02
8 34	8.194	49.186	-9.1687E 02	-8.4264E 02	-8.5385E 02	5.5905E 01	-8.2119E 02	-9.4954E 02	6.4175E 01
59.70			-1.1474E-02	3.6262E-03	1.3457E-03	2.2743E-02	7.9895E-03	-1.8118E-02	2.6108E-02
6 35	6.921	50.036	-9.8769E 02	-8.3381E 02	-8.2451E 02	2.2376E 01	-8.2150E 02	-9.9070E 02	8.4601E 01
82.33			-2.3663E-02	7.6368E-03	9.6292E-03	9.1032E-03	1.0142E-02	-2.4276E-02	3.4418E-02
7 35	7.554	50.006	-9.5181E 02	-8.4153E 02	-8.4147E 02	4.5776E 01	-8.2496E 02	-9.6833E 02	7.1685E 01
70.16			-1.7154E-02	5.2776E-03	5.2892E-03	1.8623E-02	8.6493E-03	-2.0514E-02	2.9163E-02
8 35	8.209	49.994	-9.3801E 02	-8.5972E 02	-8.6868E 02	5.2722E 01	-8.4024E 02	-9.6644E 02	6.3097E 01
61.66			-1.2218E-02	3.7103E-03	1.8877E-03	2.1448E-02	7.6710E-03	-1.7998E-02	8.6668E-02
6 36	6.927	50.734	-9.9065E 02	-8.5066E 02	-8.5681E 02	1.1235E 01	-8.5556E 02	-9.9168E 02	6.8006E 01
85.25			-2.0801E-02	7.6749E-03	6.4832E-03	4.5705E-03	6.6733E-03	-2.0991E-02	8.7668E-02
7 36	7.566	50.714	-9.7278E 02	-8.6220E 02	-8.6430E 02	3.1688E 01	-8.5572E 02	-9.8133E 02	6.2804E 01
74.85			-1.7069E-02	5.4175E-03	4.9906E-03	1.2890E-02	6.7357E-03	-1.8814E-02	8.5880E-02
8 36	8.212	50.730	-9.5325E 02	-8.7202E 02	-8.7999E 02	4.4568E 01	-8.5893E 02	-9.7431E 02	5.7699E 01
64.71			-1.2696E-02	3.8274E-03	2.2061E-03	1.8131E-02	6.4898E-03	-1.6980E-02	2.3470E-02

REPORT NO: DREV REPORT 4196/81

TITLE: 17KS12000 motor grain structural integrity analysis.

DATED: March 1981

AUTHOR: C. Carrier

SECURITY GRADING: UNCLASSIFIED Initial distribution May 1981.

1- DSIS Report Collection
Plus distribution
1- Microfiche Section (unbound copy)

1- CRAD
1- D/CRAD/L
1- D/CRAD/D
1- D/CRAD/P
1- DTA(A)
1- DTA(L)
1- DTA(M)
1- DST(OV)
1- DST(OV)-2
1- DST(OV)-3
1- DGAEM
1- DGMEM

1- DACS
1- DMCS

6- Bristol Aerospace Ltd.